

## RESEARCH ARTICLE

# Ancestral haplotype reconstruction in endogamous populations using identity-by-descent

Kelly Finke<sup>1,2</sup>, Michael Kourakos<sup>1</sup>, Gabriela Brown<sup>1</sup>, Huyen Trang Dang<sup>3</sup>, Shi Jie Samuel Tan<sup>4</sup>, Yuval B. Simons<sup>5</sup>, Shweta Ramdas<sup>6</sup>, Alejandro A. Schäffer<sup>7</sup>, Rachel L. Kember<sup>8</sup>, Maja Bućan<sup>6</sup>, Sara Mathieson<sup>4\*</sup>

**1** Department of Computer Science, Swarthmore College, Swarthmore, Pennsylvania, United States of America, **2** Department of Biology, Swarthmore College, Swarthmore, Pennsylvania, United States of America, **3** Department of Computer Science, Bryn Mawr College, Bryn Mawr, Pennsylvania, United States of America, **4** Department of Computer Science, Haverford College, Haverford, Pennsylvania, United States of America, **5** Department of Genetics, Stanford University, Stanford, California, United States of America, **6** Department of Genetics, University of Pennsylvania, Philadelphia, Pennsylvania, United States of America, **7** Cancer Data Science Laboratory, National Cancer Institute, National Institutes of Health, Bethesda, Maryland, United States of America, **8** Department of Psychiatry, University of Pennsylvania, Philadelphia, Pennsylvania, United States of America

\* [smathieson@haverford.edu](mailto:smathieson@haverford.edu)



## OPEN ACCESS

**Citation:** Finke K, Kourakos M, Brown G, Dang HT, Tan SJS, Simons YB, et al. (2021) Ancestral haplotype reconstruction in endogamous populations using identity-by-descent. *PLoS Comput Biol* 17(2): e1008638. <https://doi.org/10.1371/journal.pcbi.1008638>

**Editor:** Degui Zhi, University of Texas Health Science Center at Houston, UNITED STATES

**Received:** May 1, 2020

**Accepted:** December 15, 2020

**Published:** February 26, 2021

**Copyright:** This is an open access article, free of all copyright, and may be freely reproduced, distributed, transmitted, modified, built upon, or otherwise used by anyone for any lawful purpose. The work is made available under the [Creative Commons CC0](https://creativecommons.org/licenses/by/4.0/) public domain dedication.

**Data Availability Statement:** Our software thread is available open-source at <https://github.com/mathiesonlab/thread>. Researchers can run our method on their own dataset using this code, or they can apply to access the genotype data from an Old Order Amish population which we utilize, which is governed by IRB protocol #827037 at the University of Pennsylvania. As this Amish population is a genetic isolate, individual level data is not shared publicly to maintain privacy for this community. Additionally, although access to the Anabaptist Genealogy Database (AGDB) is not

## Abstract

In this work we develop a novel algorithm for reconstructing the genomes of ancestral individuals, given genotype or sequence data from contemporary individuals and an extended pedigree of family relationships. A pedigree with complete genomes for every individual enables the study of allele frequency dynamics and haplotype diversity across generations, including deviations from neutrality such as transmission distortion. When studying heritable diseases, ancestral haplotypes can be used to augment genome-wide association studies and track disease inheritance patterns. The building blocks of our reconstruction algorithm are segments of Identity-By-Descent (IBD) shared between two or more genotyped individuals. The method alternates between identifying a source for each IBD segment and assembling IBD segments placed within each ancestral individual. Unlike previous approaches, our method is able to accommodate complex pedigree structures with hundreds of individuals genotyped at millions of SNPs.

We apply our method to an Old Order Amish pedigree from Lancaster, Pennsylvania, whose founders came to North America from Europe during the early 18th century. The pedigree includes 1338 individuals from the past 12 generations, 394 with genotype data. The motivation for reconstruction is to understand the genetic basis of diseases segregating in the family through tracking haplotype transmission over time. Using our algorithm *thread*, we are able to reconstruct an average of 224 ancestral individuals per chromosome. For these ancestral individuals, on average we reconstruct 79% of their haplotypes. We also identify a region on chromosome 16 that is difficult to reconstruct—we find that this region harbors a short Amish-specific copy number variation and the gene *HYDIN*. *thread* was developed for endogamous populations, but can be applied to any extensive pedigree with the recent generations genotyped. We anticipate that this type of practical ancestral

required to reproduce the analyses in this work, interested researchers must have an IRB-approved protocol to study an Anabaptist population and may contact Dr. Leslie Biesecker at [lesb@mail.nih.gov](mailto:lesb@mail.nih.gov).

**Funding:** KF is funded by a Robbins/Chang Summer Fellowship. ST is funded by a Kovaric Fellowship. YBS is funded by NIH grant no. 1F32HG011202-01. AAS is funded by the Intramural Research Program of the National Institutes of Health, National Cancer Institute. MB is supported in part by the NIH grant R01MH093415. This work utilized the computational resources of the NIH HPC Biowulf cluster <http://hpc.nih.gov>. The funders had no role in study design, data collection and analysis, decision to publish, or preparation of the manuscript.

**Competing interests:** The authors have declared that no competing interests exist.

reconstruction will become more common and necessary to understand rare and complex heritable diseases in extended families.

## Author summary

When analyzing complex heritable traits, genomic data from many generations of an extended family increases the amount of information available for statistical inference. However, typically only genomic data from the recent generations of a pedigree are available, as ancestral individuals are deceased. In this work we present an algorithm, called `thread`, for reconstructing the genomes of ancestral individuals, given a complex pedigree and genomic data from the recent generations. Previous approaches have not been able to accommodate large datasets (both in terms of sites and individuals), made simplifying assumptions about pedigree structure, or did not tie reconstructed sequences back to specific individuals. We apply `thread` to a complex Old Order Amish pedigree of 1338 individuals, 394 with genotype data.

This is a *PLOS Computational Biology Methods* paper.

## Introduction

Pedigree structures and associated genetic data provide a wealth of information for studying recent evolution. Nuclear families (parents and children) and other small pedigrees have been used to estimate mutation and recombination rates in humans [1–4] and other species [5–7]. Pedigrees have informed breeding of domesticated animals [8], enabled the study of short-term evolution in natural populations [9], and can be used to study heritable diseases [10].

Genetic studies of rare, recessive traits pose a challenge to researchers when individuals expressing these traits are too sparse or too scattered to obtain sufficient genetic data. Endogamous populations with detailed pedigree records provide an important exception. Endogamous populations, defined by the practice of marriage within a social, ethnic, or geographic group, are often characterized by small effective population sizes with limited external admixture. These groups are of great interest to geneticists because a single small population can provide enough data to inform rare trait and rare variant studies with worldwide implications [11, 12]. Endogamous populations are also informative for common diseases [13, 14].

Extended pedigrees from endogamous populations provide a valuable system for studying heritable disease, but genetic data is typically limited to recent generations. If genetic information from every individual in the pedigree were available, we would be in a better position to understand the transmission of disease-associated variants throughout the history of the population. More specifically, we often know the disease phenotypes of ancestral individuals, but cannot obtain their genetic information. In these cases, reconstructed haplotypes would allow us to augment genome-wide association studies (GWAS), where large sample sizes are essential. In addition, reconstructed genomes would enable the computation of polygenic risk scores (PRS) [15, 16] for ancestral individuals.

Reconstructed ancestral haplotypes also allow us to study genome dynamics over short time scales, including inheritance patterns and haplotype transmission. In populations with large nuclear families, transmission distortion [17, 18] and other deviations from neutrality are particularly visible. Understanding which parts of the genome are over- or under-represented in the recent generations could help us identify forms of deleterious variation. From a theoretical perspective, there has been relatively little work on the question of how much ancestral reconstruction is possible given genetic information from contemporary individuals. One example from a small livestock pedigree can be found in [19].

Previous work on ancestral reconstruction has typically been applied to small pedigrees with no *loops* (marriage between close relatives). One of the earliest examples comes from the Lander-Green algorithm [20], which uses a hidden Markov model (HMM) with inheritance vectors as the hidden state and genotypes as the observed variables. Methods such as *SimWalk2* [21] and *Merlin* [22] use descent graphs and sparse gene flow trees (respectively) to extend the idea of likelihood-based computation to larger pedigrees. However, these methods do not perform reconstruction explicitly and also do not handle loops, as tree-based intermediate steps are common to both algorithms. With millions of loci and hundreds of individuals, the time complexities of these methods are prohibitive (see [23] for a runtime overview). Other HMM-based approaches such as *HAPPY* [24], *GAIN* [25], and *RABBIT* [26] reconstruct genome ancestry blocks, but do not tie them to specific individuals. *HAPLORE* [27] quantifies possible ancestral haplotype configurations but does not incorporate recombination, and the Bayesian approach in [28] is more suitable for haplotyping.

The authors of [29] reconstructed ancestral haplotypes for the purpose of identifying regions that contain susceptibility genes for schizophrenia. However, their pedigree was much smaller (with no loops), many fewer markers (450) were used, and several of the reconstruction steps were done by inspection or by hand, which does not scale to our scenario. Another study [30] reconstructed the African haplotype of an African-European individual who migrated to Iceland in 1802 and had 788 descendants, 182 of which were genotyped. However, this scenario is much simpler, as the regions of African ancestry within each descendant were easily identified and all belonged to the same individual.

The problem studied here is different from *pedigree reconstruction*, where genetic information is used to reconstruct (previously unknown) family relationships (see [31–36]). It is also different from ancestral reconstruction in a phylogenetic context, where a single tree represents the evolutionary relationships between species (see [37]).

In this study we apply our method to an Old Order Amish population from Lancaster, Pennsylvania who can trace their ancestry to founders who came from Europe to Philadelphia in the early 18th century (see Fig 3 of [38] for an analysis of the contributions of the 554 founders). The Amish are an ethno-religious group in the Anabaptist tradition, with a history of detailed record keeping and marriage within the Amish community [39]. In this work, we study an unpublished pedigree of 1338 individuals, augmented [40] from a pedigree of 784 individuals originally described in the Amish Study of Major Affective Disorder [41, 42]. Roughly one third of the individuals in the original pedigree display some form of mood disorder, and about 19% have been diagnosed with bipolar disorder specifically [16]. Bipolar disorder in a broad sense is roughly 80% heritable in this pedigree [16], and recent work has focused on understanding the genetic basis of this disease [42]. The availability of genetic data from 394 contemporary individuals from this pedigree gives us an opportunity to use reconstruction as another lens on inheritance patterns of mood disorders.

Here we present a novel algorithm, *thread*, for reconstructing ancestral haplotypes given an arbitrary pedigree structure and genotyped or sequenced individuals from the recent generations. *thread* can be applied in a variety of scenarios including pedigrees with loops,

inter-generational marriage, and remarriage. More ancestral chromosomes will be reconstructed as the percentage of individuals with genetic data increases, but our method can be applied even when this fraction is modest. This work represents a key step towards understanding the limits of quantifying the genomes of ancestral individuals in the absence of ancient DNA. `thread` is available as an open-source software package: <https://github.com/mathiesonlab/thread>.

## Materials and methods

### Ethics statement

All work contained within this study was approved by the IRB of the Perelman School of Medicine at the University of Pennsylvania (protocol #827037). All study participants were 18 years or older and provided written consent (see [42] for details of the consent process). The Anabaptist Genealogy Database (AGDB) [40] is covered by an IRB-approved protocol at the NIH (protocol #97HG0192).

### Problem statement

The first input to our reconstruction algorithm `thread` is a pedigree structure  $\mathcal{P}$ . For each individual  $p \in \mathcal{P}$  (aside from founders and married-in individuals), we have information about the mother  $p^{(m)}$  and father  $p^{(f)}$ , which are also members of  $\mathcal{P}$ . In the case of founders or married-in individuals, we represent  $p^{(m)}$  and  $p^{(f)}$  as 0's. The pedigree may contain loops. Formally, a loop occurs when the undirected version of the directed marriage graph has a cycle (see [43, 44] for more information). Usually a loop means that the parents of a child share a common ancestor, but other loop structures are possible, e.g. when two brothers marry two sisters.

The second input is a dataset of phased haplotypes (e.g. in Variant Call Format, VCF) from a subset of individuals in the pedigree, typically from the most recent generations. Phasing assigns the alleles of each individual to parental haplotypes. Our aim is to reconstruct the haplotypes of as many ancestral individuals in the pedigree as possible. An illustration of the problem is shown in Fig 1.

### High level description

`thread` is built upon the idea of Identity-By-Descent (IBD). IBD segments are long stretches of DNA shared by a *cohort* of two or more individuals due to descent from a common ancestor (*source*). Our algorithm alternates between analyzing IBD segments and analyzing individuals. During each iteration (outer loop of Algorithm S1), we first consider each IBD segment independently (as opposed to working sequentially along the chromosome as an HMM would). We attempt to find the source of the IBD segment, as well as individuals who are on descent paths from this ancestor to the cohort. After source identification we consider each individual in turn, clustering and assembling their associated IBD segments into haplotypes. During this grouping step we identify IBD segments that have been placed in a manner that is inconsistent with assigned haplotypes—in the next iteration we will update their sources. We repeat these steps until no new haplotypes are reconstructed. Each chromosome of the genome is processed independently. A schematic of `thread` is shown in Fig 2, and pseudocode is given in Algorithm S1 (S1 Text).

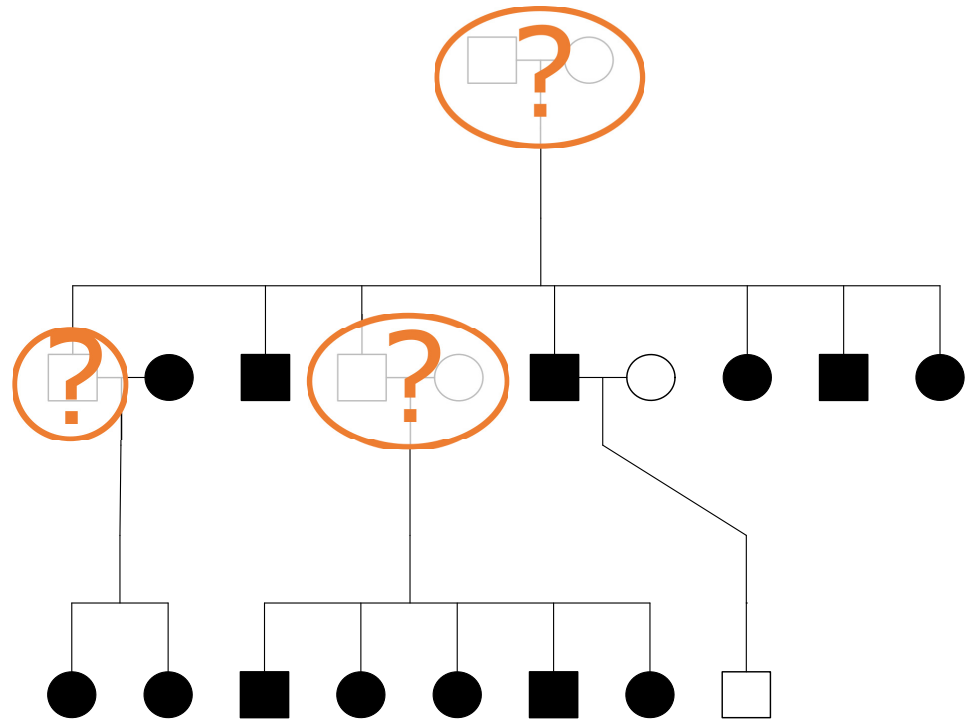


**Fig 1. Problem statement illustration.** Squares represent males and circles represent females. Horizontal lines create couples and show sibling relationships. Parents and offspring are connected by vertical lines. Filled in symbols represent individuals who have been genotyped. Our aim is to reconstruct all ungenotyped individuals (orange question marks) who have genotyped descendants.

<https://doi.org/10.1371/journal.pcbi.1008638.g001>

**Input:** sequence data for subset of individuals and pedigree structure

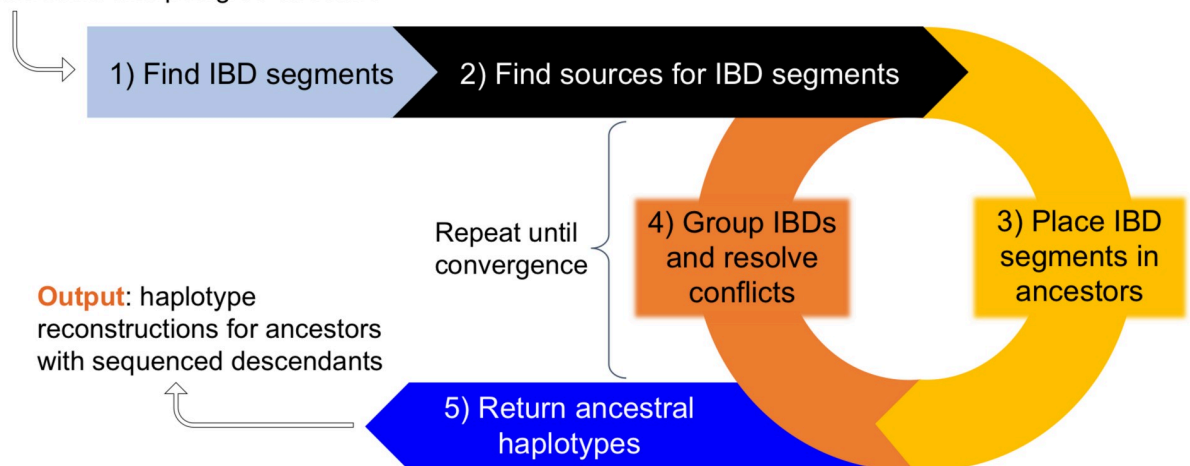


**Fig 2. Algorithm overview.** In the first two steps we identify IBD segments and compile a list of potential sources for each one. In the iterative phase, we alternate between choosing sources for each IBD and grouping the IBDs that are placed within each individual. If the IBDs assigned to an individual can be arranged into two haplotypes meeting thresholds for coverage defined in Methods, then those haplotypes are considered *strong*. IBD segments that conflict with strong haplotypes are rejected and must be assigned a different source. When we are no longer building more haplotypes, we return the reconstructed chromosomes.

<https://doi.org/10.1371/journal.pcbi.1008638.g002>

**Table 1. Individuals per generation, with the founders assigned generation 1.** The generation of a non-founder is defined to be one more than the maximum of the generations of their parents. Married-in individuals carry the generation of their spouse. The total number of individuals is 1338, with genotype information for 394 (largely in generations 9–12).

Generation	# Individuals	# Genotyped
1	9	0
2	15	0
3	35	0
4	64	0
5	76	0
6	149	0
7	186	0
8	187	4
9	142	53
10	198	143
11	178	145
12	99	49

<https://doi.org/10.1371/journal.pcbi.1008638.t001>

## Input pedigree

The Amish pedigree under study was developed from several sources, including the book *Descendants of Christian Fisher* [45], the Anabaptist Genealogy Database (AGDB) [40] and associated software `PedHunter` [38], and the Amish Study of Major Affective Disorder [41]. A summary of the number of individuals in each generation is shown in Table 1, along with the number of genotyped individuals. The complete pedigree structure is shown in S1 Fig (created with the `kinship2` R package [46]).

To assess the levels of relatedness and genetic similarity in this population, we compare the haplotypes of each pair of genotyped individuals. For each comparison, we compute the number of SNPs two haplotypes have in common over the total number of genotyped SNPs. Then for each pair of individuals, we take their overall genetic similarity to be the average of their haplotype similarities (paired to maximize similarity). This method accounts for differing chromosome lengths by weighting the similarities based on the number of SNPs genotyped on each chromosome. We plot genetic similarity against kinship coefficient, which is computed using `PedHunter` and the AGDB (or our Amish pedigree if one or both of the individuals are not in the AGDB). The results are shown in Fig 3, which demonstrates that genetic similarity generally increases linearly as kinship coefficient increases. We also include a histogram of inbreeding coefficients for each individual in S2 Fig (also computed using `PedHunter`). See [47] for more information about kinship and inbreeding coefficients.

## Step 1: Find IBD segments

Step 1 begins by reading in the pedigree structure. The pedigree may contain inter-generational marriage and loops, and the individuals do not need to be separated into generations. Let  $t$  be the total number of individuals in the pedigree,  $n$  be the number of genotyped individuals, and  $m$  be the number of ungenotyped individuals with genotyped descendants. In the pedigree under study,  $t = 1338$ ,  $n = 394$ , and  $m = 686$ , leaving 258 individuals with no genotyped descendants; we do not expect to be able to reconstruct these individuals.

Next, IBD segments between pairs of genotyped individuals are identified using `GERMLINE` [48], although `IBD-Groupon` for detecting IBD in groups could be used instead [49]. When using `GERMLINE`, we use the default parameters, except for the `-haploid` flag to



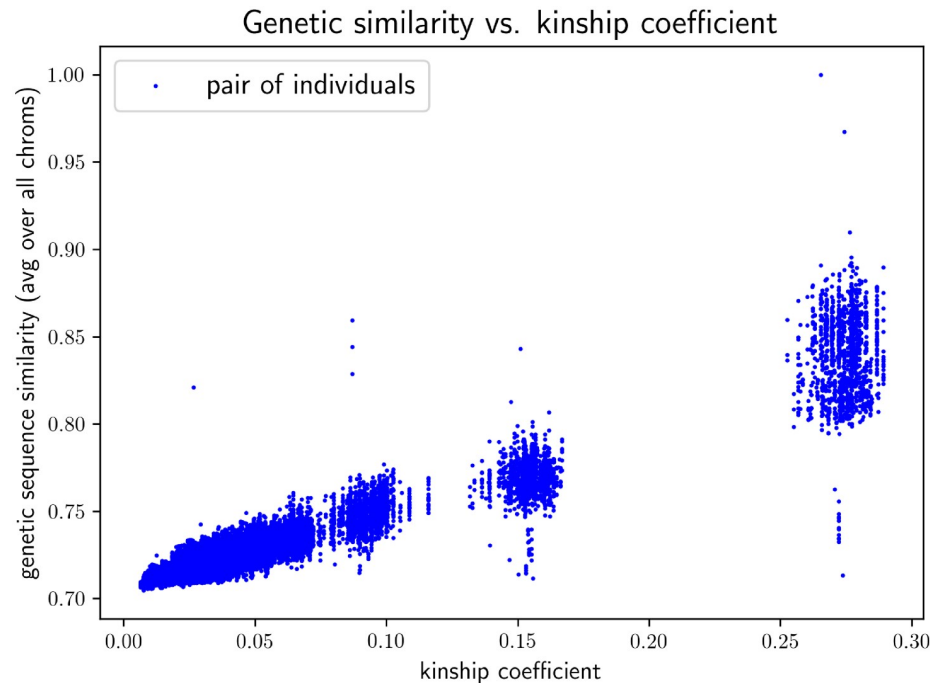


**Fig 3. Genetic similarity vs. kinship.** For each pair of genotyped individuals, we compute their genetic similarity (counting genotyped SNPs only) and plot this on the  $y$ -axis against their kinship coefficient on the  $x$ -axis. The expected linear trend is apparent, with an average sequence similarity of 72.5%. The minimum similarity out of all pairs was 70.5%, and the maximum was 99.999% (twins).

<https://doi.org/10.1371/journal.pcbi.1008638.g003>

indicate our dataset is phased. Thus the minimum IBD segment length is 3cM, and the length of seeds for exact matches is 128 markers. For each IBD segment  $I$ , we combine pairs until we obtain a cohort  $C$  of individuals who share this segment, where  $|C| \in \{2, n\}$ . The *descendance path* of an IBD segment includes all descendants of the source who also passed down the IBD to reach the cohort descendants. In this Amish pedigree, genotypes for each genotyped individual were obtained from Illumina Omni 2.5M SNP arrays, and then phased into haplotypes using SHAPEIT2 [50]. The size of  $C$  ranged from two to 180 individuals.

## Step 2: Find sources for IBD segments

In the next phase of `thread`, sources for each IBD segment are identified independently. By the end of this step, we will have enumerated all possible individuals who could have been the source of each IBD segment  $I$ , given its associated cohort  $C$ . This process is done only once and is not part of the iterative phase. When searching for *all* common ancestors of a cohort, each previous generation doubles the number of ancestors to search. `thread` maximizes efficiency in this exponential problem by merging overlapping paths using a modified breadth-first search algorithm (explained in detail below and in pseudocode in Algorithm S2).

First all the individuals in the cohort are added to a queue. For example, in Fig 4,

$$C = \{1, 2, 5, 7, 8\}$$

so we would start out with  $Q = (1, 2, 5, 7, 8)$ . We then pop the first individual,  $p_0 = 1$  (in this example), off the queue. If  $p_0$  is an ancestor of all individuals in the cohort, we add  $p_0$  to a set of possible sources,  $S$ . Either way, we add  $p_0$ 's parents to the back of the queue and keep processing individuals (even if  $p_0$  is an ancestor, its parents may be ancestors via paths that do not

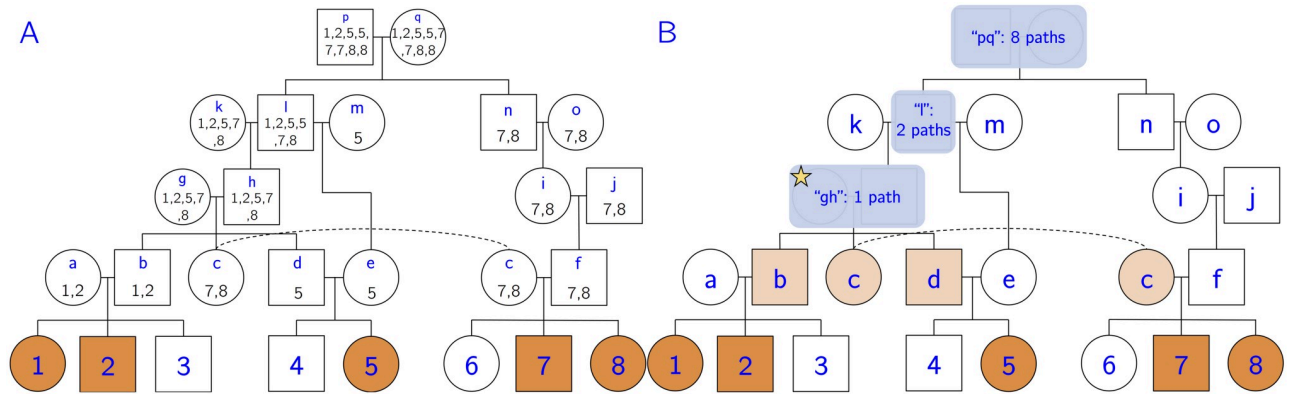


**Fig 4. Source-finding illustration.** (A) Let individuals 1–8 be the genotyped individuals of this pedigree. Let  $C = \{1, 2, 5, 7, 8\}$  (orange individuals) be the cohort sharing IBD segment  $I$ . Note that this pedigree contains two loops, since  $c$  and  $f$  share recent ancestors  $p$  and  $q$ , and  $d$  and  $e$  share recent ancestor  $l$ . The multiset  $M_p$  for each ancestral individual  $p$  is shown below the node name.  $M_p$  is formed by concatenating the multisets of  $p$ 's children, and it represents the number of paths from ancestor  $p$  to each member of the cohort. (B) After trimming redundant ancestors and merging couples, we obtain a set of putative sources for the IBD segment. In this case, we have three potential sources:  $S = \{gh, l, pq\}$ . We begin the iterative phase by selecting the source with the fewest descendance paths, which in this case is  $gh$  (starred). We place the IBD segment in individuals that are on all paths from  $gh$  to the cohort. In this case we would add the IBD segment to individuals  $b, c$ , and  $d$  (light orange).

<https://doi.org/10.1371/journal.pcbi.1008638.g004>

include  $p_0$ ). In this example, we first pop individual 1 off the queue. Since it has not been processed, we push 1's parents onto the end of the queue to obtain

$$Q = (2, 5, 7, 8, a, b).$$

Each time we add an individual  $p$  to the queue, we keep track of how many paths exist from  $p$  to the members of the cohort using a multiset  $M_p$ . For the members of the cohort,  $M_p = \{p\}$  (just one path to themselves). When we add a parent to the queue, we concatenate the multisets of the individual's children. For individual  $a$  in this example, its multiset would become  $M_a = \{1, 2\}$ , indicating one path to individual 1 and one path to individual 2. Going further up the pedigree, individual  $l$  has two children,  $h$  and  $e$  with  $M_h = \{1, 2, 5, 7, 8\}$  and  $M_e = \{5\}$ . Concatenating these two multisets, we obtain the multiset  $M_l = \{1, 2, 5, 5, 7, 8\}$ , indicating that there are two possible paths from  $l$  to cohort member 5. As soon as an individual's multiset contains all members of the cohort, the individual is a possible source.

There are two post-processing phases to the source-finding algorithm. (1) Trim redundant sources: a source is redundant if it is an ancestor of another source and does not add any unique descendance paths to the cohort. In other words, we do not want to include individuals if *all* their paths to the cohort go through another source. Redundant sources do not depend on ordering effects, other than that children are added to the queue before their parents. Formally, if the cardinality of an individual's multiset is equal to the maximum cardinality of the multisets of its children, it is redundant (for example,  $k$  is a redundant ancestor since  $|M_k| = |M_h|$ ). (2) We merge couples into a single source, as typically we will not be able to resolve the source of an IBD segment beyond the couple level. Spouses with different multiset cardinality are an exception. These cases are usually caused by remarriage with at least one child from each marriage. Individual  $l$  is an example; we do not consider couple  $kl$  a source because  $|M_k| < |M_l|$  due to  $l$ 's remarriage to  $m$ . If the cardinalities had been the same (and not redundant), we would have considered  $kl$  a source.

In the Fig 4 example, we identify three potential sources:  $S = \{gh, l, pq\}$ . Note that we cannot stop processing the queue when we get to source  $gh$ , as there exist sources further up the pedigree that are in previously unvisited descendance paths.



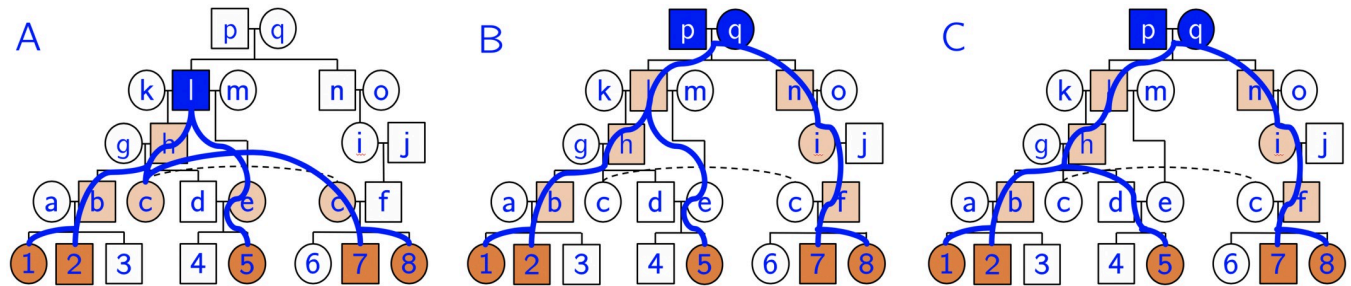


**Fig 5. Example descent paths.** Given a cohort of five individuals sharing an IBD segment (orange), we often obtain multiple sources (blue nodes) and multiple descent paths (blue lines) from each source. In this example we have 11 total paths from three sources. After we choose a source, we assign the IBD segment to ancestors along *all* descent paths (light orange). (A) One path from source  $\ell$ . (B)-(C) Two different descent paths from the same source  $pq$ . We would not assign the IBD to  $d$  and  $e$  since they are not on all paths from this source.

<https://doi.org/10.1371/journal.pcbi.1008638.g005>

The use of multisets allows us to quickly determine the number of descent paths from each source to the cohort. For each source  $s$  and each individual  $c$  in the cohort, let  $m_s(c)$  be the multiplicity of  $c$  in  $M_s$ . For example, in  $M_\ell$ , the multiplicity of individual 5 is two, meaning that there are two paths from  $\ell$  to individual 5. The total number of descent paths ( $d$ ) from source  $s$  to cohort  $C$  (sharing IBD  $I$ ) is the product of all the multiplicities:

$$d(s) = \prod_{c \in C} m_s(c)$$

In this example, we obtain  $d(gh) = 1$ ,  $d(\ell) = 2$ , and  $d(pq) = 8$ . A few of these descent paths are shown in blue in Fig 5 for clarity.

Before moving into the iterative part of the algorithm, we take note of individuals that are on *all paths from all sources*. For example, individual  $b$  happens to be on all 11 paths from the sources, so we know that individual  $b$  should have the IBD segment.

### Step 3: Place IBD segments in ancestors

At this stage the iterative part of the algorithm begins. Every iteration starts with lists of *reconstructed* individuals and *unreconstructed* individuals. During the first iteration, the *reconstructed* list only includes genotyped individuals. The goal of Step 3 is to select a source for each IBD segment out of the potential sources enumerated in Step 2. While the true source is unknown at this stage, we provide two methods for selecting a likely source.

For the first method, we use the greedy heuristic of choosing the source with the fewest paths, provided that it does not create a conflict with one of the *reconstructed* individuals. The intuition behind choosing the source with the fewest paths is that this source will (often) be more recent than others, with fewer meioses separating the source from the cohort. For example, in Fig 4, we would choose source  $gh$  since it has only one descent path. We denote this method “min path”.

An alternative approach involves computing the probability that an IBD segment is transmitted from the source to all members of the cohort, taking into account the length of the IBD segment and the genetic map. We then select the source with the highest probability. If this source is rejected due to IBD conflicts in the grouping stage (Step 4), we take the source with the next highest probability. Although we track the probability of IBD transmission throughout the paths from the source to the cohort, we do not account for the probability that non-cohort members do *not* have the IBD. Therefore these computations do not result in the probability of observing a particular configuration of the segregating IBD segment, only the

probability of transmission to the cohort. We denote this method “max prob” (further mathematical details are provided in [S1 Text](#), under the *Probabilistic source identification* section).

Once a source is selected, we can begin to look at the individuals that lie on paths from this source. In the case of only one path, all the individuals on the path will be given the IBD segment ( $b$ ,  $c$ , and  $d$  in this example), thus augmenting the associated cohort. In the more common situation when we have multiple paths from the source, we give the IBD segment only to individuals that appear on *all* the paths. However, if we try to give this IBD segment to a *reconstructed* individual and it conflicts with both of the individual’s previously assigned haplotypes, we reject the source and choose the source with the next fewest paths or next highest probability. These tentative assignments result in potentially conflicting IBDs being assigned to the same individual, which we resolve in Step 4.

#### Step 4: Group IBDs and resolve conflicts

During Step 3, we analyzed each IBD segment independently, identifying ancestral individuals who likely also share the IBD segment. In Step 4, we analyze the *individuals* independently and assemble the IBDs that have been placed within each individual. Say we are analyzing ancestral individual  $p$  with putative set of IBD segments  $\mathcal{I}_p$ . The goal of assembly is to separate the IBD segments into two haplotypes such that their sequences are consistent within each group. At a high level, this process can be compared to *de novo* genome assembly, where many small reads are stitched together to create contigs. We have an advantage over traditional assembly because we know the locations of each segment along the chromosome. But we may have included IBD segments that do not actually belong to a given individual, which we will need to identify and remove.

After grouping, we can identify individuals that are *reconstructed*. We define reconstructed as follows.

**Definition 1.** *Reconstructed individual.* If we can group the IBDs placed within an individual into exactly two *strong* groups, we declare the individual *reconstructed*. Additionally, if there are two strong groups plus additional groups, the groups that are not strong must either have half as many IBD segments or be half as long as the weaker of the two strong groups.

**Definition 2.** *Strong group.* To determine if a group is *strong*, it must meet a combination of thresholds: a minimum number of IBD segments and a minimum coverage (#SNPs reconstructed/#SNPs genotyped on the chromosome). We use a sliding scale: if the group contains 1-2 IBDs, it must cover 90% of the SNPs. If a group contains 3-9 IBDs, it must cover 70% of the SNPs. And if a group contains 10 or more IBDs, it must cover 50% of the SNPs. These parameters can be customized by the user.

Our grouping algorithm (covered in pseudocode in Algorithm S3) begins by identifying regions of homozygosity within the IBD segments. This is accomplished by condensing all segments in  $\mathcal{I}_p$  down into a single sequence with a list of alleles at each site. Any region greater than 300kbp with only one allele per site and at least 100 SNPs is declared homozygous. It is important to identify these regions early in the grouping algorithm, otherwise we may assume only one group contains this stretch. Each homozygous region is duplicated so that each chromosome will have a copy, and IBD segments contained within homozygous regions are not used in the next stages.

We process the remaining IBDs (those not incorporated into a group) one by one, from longest to shortest (in kbp). If the IBD does not overlap with any of the current groups, we create a new group initialized by the IBD segment. If the IBD does overlap with one or more groups, we add it to the group with the largest overlap (above a threshold).

At this point in the grouping algorithm, we have a set of homozygous groups, a set of heterozygous groups, and a set of remaining IBDs. If an IBD overlaps with two groups, we use it to merge the groups into one (assuming no previous overlap/conflict). Finally, we merge groups that “line up” with each other—i.e. they do not overlap, but their IBD segments span adjacent SNPs and were likely separated by an ancestral recombination event. At the end of this process, three situations may emerge:

- We have two clear groups (which meet our definition of *strong*) forming two haplotypes. This is the ideal scenario and it means we have a successful reconstruction of the individual.
- We have two strong groups, but we also have several weaker ones. This scenario is resolvable, as we can retain the two strong groups as the reconstruction, and reject the other groups. The IBD segments from the rejected groups give us a lot of information—since this individual was on *all* paths from the selected source, if the IBD segment does not fit with the reconstructed haplotypes, then we assume the source was incorrect. Throughout Step 4 we collect all IBD segments that have been incorrectly sourced to update in the next iteration.
- In all other situations, we typically cannot resolve the individual’s haplotypes. We may have only one group (which could be one of the individual’s haplotypes), but we do not declare the individual reconstructed. We could have many groups without two strong ones, or we may not have assigned any IBDs to the individual.

At the end of Step 4, we move individuals from the first two scenarios in to the *reconstructed* list. IBDs that did not cause any conflicts are marked as processed and we retain the rest to re-source in the next iteration. An illustration of the grouping algorithm is shown in Fig 6.

### Step 5: Return ancestral haplotypes

At the end of Step 4 we have a set of IBD segments that were incorrectly sourced. We then repeat Step 3: we update the source for each such IBD by selecting the source with the next fewest paths. This allows us to assign the IBD to a new set of individuals. In the next Step 4 we treat reconstructed individuals and unreconstructed individuals differently. If an individual is

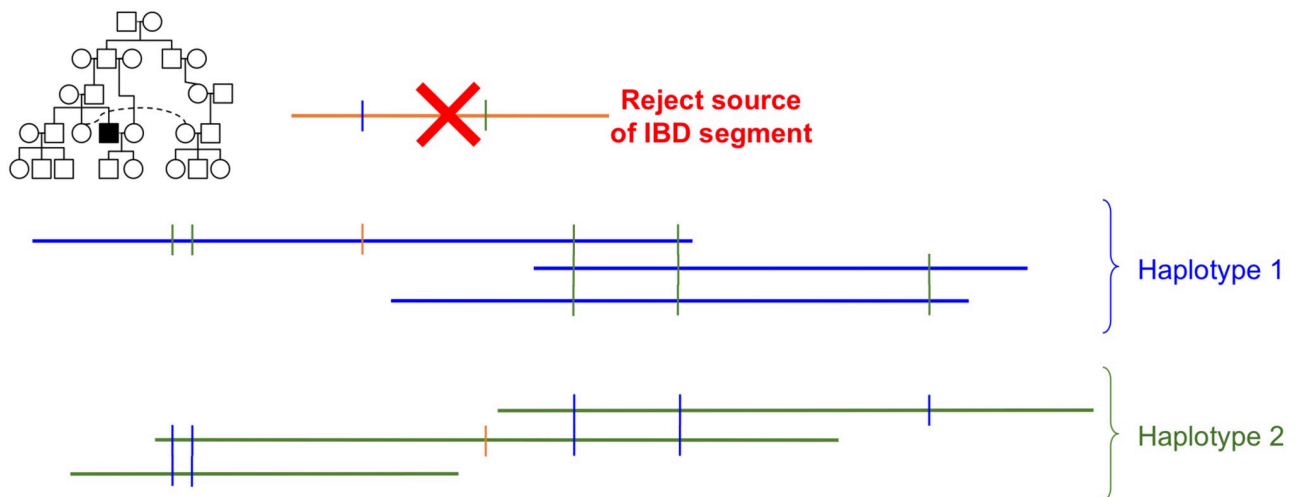


**Fig 6. Grouping algorithm illustration.** Each horizontal line represents one IBD segment that we placed within a specific individual (highlighted in the pedigree inset). Each vertical line indicates a difference (heterozygous site) between groups. In this case, the orange IBD segment conflicts with both the blue and green groups, so we would reject its source and attempt to find a new one in the next iteration.

<https://doi.org/10.1371/journal.pcbi.1008638.g006>

already marked as reconstructed, we use each additional IBD to strengthen its groups or reject the new source of the IBD. If an individual has not been reconstructed, we run the grouping algorithm again. We keep iterating Steps 3 and 4 until we are no longer reconstructing more individuals.

The final step is to return the haplotype sequences for the reconstructed individuals. These may contain some gaps, but due to our coverage and length thresholds, if an individual is declared reconstructed, we will return at least half of each haplotype (for the chromosome under consideration). In [S1 Text](#) we provide a theoretical complexity analysis of the full algorithm.

## Validation

We used two approaches to validate our approach directly. (1) To test the grouping algorithm, we grouped all IBD segments identified (by `GERMLINE`) as belonging to each *genotyped* individual. For this process, we did not specify which IBD segments belonged to which haplotypes, even though this information is known for genotyped individuals. (2) To evaluate our reconstruction results under a realistic situation, we “left-out” one genotyped individual at a time and attempted to reconstruct that individual’s genome. We restricted this analysis to genotyped individuals with at least one genotyped descendant, which left 89/394 individuals. Because all the genotyped individuals are in the five most recent generations, this analysis is limited to the more recent past. This approach can be interpreted as a form of leave-one-out cross-validation. In both of these validation approaches we compared the reconstructions to the original haplotypes using sequence similarity.

We also validated our method through whole-genome simulations. To mirror the demographic history of the Amish, we first simulated a founder population using `msprime` [51] with an effective population size of 10,000 diploids and the HapMap recombination map [52]. To simulate pre-migration endogamy in Europe, we created a 25-generation pedigree structure with a small constant population size (400 diploids). In this pedigree structure we constrained 5% of marriages to be between second-degree relatives (e.g. first-cousins), 10% between third-degree relatives, and 10% between fourth-degree relatives. We used `Ped-sim` [53] to simulate genetic data under this pedigree, using sequences from `msprime` as the founders. In the final generation of this pre-migration phase, we were left with genetic data for 400 individuals, 186 of which we use as founders for the true Amish pedigree structure after migration to North America. We again used `Ped-sim` to create genetic data for the 1338 individuals in this pedigree, and retained this data for the same 394 individuals we have genotyped. Finally, we ran `GERMLINE` and `thread` on this dataset, and compared the reconstructed sequences to their true values.

We also developed a method to automatically predict which individuals would be well reconstructed. To do this, we created a filter that identifies individuals based on their generation and average per-base IBD coverage, since we find that more recent individuals and those with high IBD coverage are typically more accurately reconstructed. In the Results section we highlight how many individuals pass this filter and the average reconstruction accuracy of these individuals.

Our simulation framework provides the opportunity to test `thread` in a variety of scenarios. First, to model varying levels of endogamy, we varied the size of the pre-migration population from 200 to 2000 individuals. Additionally, we compared our first IBD source identification algorithm “min path” (greedy approach of taking the source with the fewest paths to the cohort) with the probabilistic approach “max prob” (described in Step 3 and in [S1 Text](#)).

By using IBD segments called by GERMLINE, the input to `thread` may already contain inaccuracies from segments that are Identical-By-State (IBS). To assess the impact of such inaccuracies, we used the true IBD segments as input to `thread`. These true IBD segments are identified by `Ped-sim` as part of simulating meiosis. These segments reflect IBD post-migration; there may be more ancient IBD sharing not reflected in the `Ped-sim` segments. In addition, it is possible that some individuals in the population share a known IBD segment due to IBS, but are not included in the `Ped-sim` segments because they did not inherit the segment from an ancestor in the pedigree.

Finally, our simulation framework allowed us to experiment with the strong groups definition, as a single definition of strong group may not be applicable for all individuals across all generations. To that end, we tested two different settings of the strong group definition.

- Setting A: For individuals with generation number 8 or greater, we use the same strong group settings as before. If the individual has generation number 7 or lower (i.e. more ancient) then we use the following sliding scale: if the group contains 1-3 IBDs, it must cover 90% of the SNPs. If a group contains 4-14 IBDs, it must cover 70% of the SNPs. And if a group contains 15 or more IBDs, it must cover 50% of the SNPs. This is meant to provide stricter thresholds for individuals in the more ancient generations.
- Setting B: For individuals with generation number 8 or greater, we use the same strong group settings as before. If the individual has generation number 7 or lower (i.e. more ancient) then we use the following sliding scale: if the group contains 1-3 IBDs, it must cover 70% of the SNPs. If a group contains 4-14 IBDs, it must cover 60% of the SNPs. And if a group contains 15 or more IBDs, it must cover 50% of the SNPs. This is meant to relax the IBD length thresholds, but still require more IBD segments for individuals in the more ancient generations.

## Results

### Grouping algorithm validation

After grouping the IBD segments called for each genotyped individual of the Amish pedigree, we analyzed the resulting haplotypes for coverage and correctness. [Fig 7](#) shows two chromosomes of a *genotyped* individual that were reconstructed using the grouping algorithm `thread`. Each horizontal line represents one IBD segment shared with a cohort of other genotyped individuals. IBD segments of the same color represent haplotypes, and have a consistent sequence along the chromosome. In other words, if we agglomerated the IBD segments of a single color in [Fig 7A](#) or [Fig 7B](#), a single sequence would emerge. In general we found that our grouping algorithm worked very well for genotyped individuals, who typically share many IBD segments with other members of the pedigree. In 8558 out of 8668 chromosomes (22 per genotyped individual), we successfully grouped placed IBDs into two haplotypes. Very occasionally (1.3% of cases) we obtained three groups (example in [Fig 7A](#)). In chromosome 21 for one individual, all IBD segments belonged to a single group, indicating homozygosity along the entire chromosome. The sequences of these grouped haplotypes are very close to the true haplotypes—average per chromosome accuracies are between 98.6% and 99.7%, as measured by sequence similarity.

### Leave-one-out validation

To evaluate our reconstruction results under a realistic situation, we “left-out” one genotyped individual at a time and attempted to reconstruct that individual’s genome. We restricted this



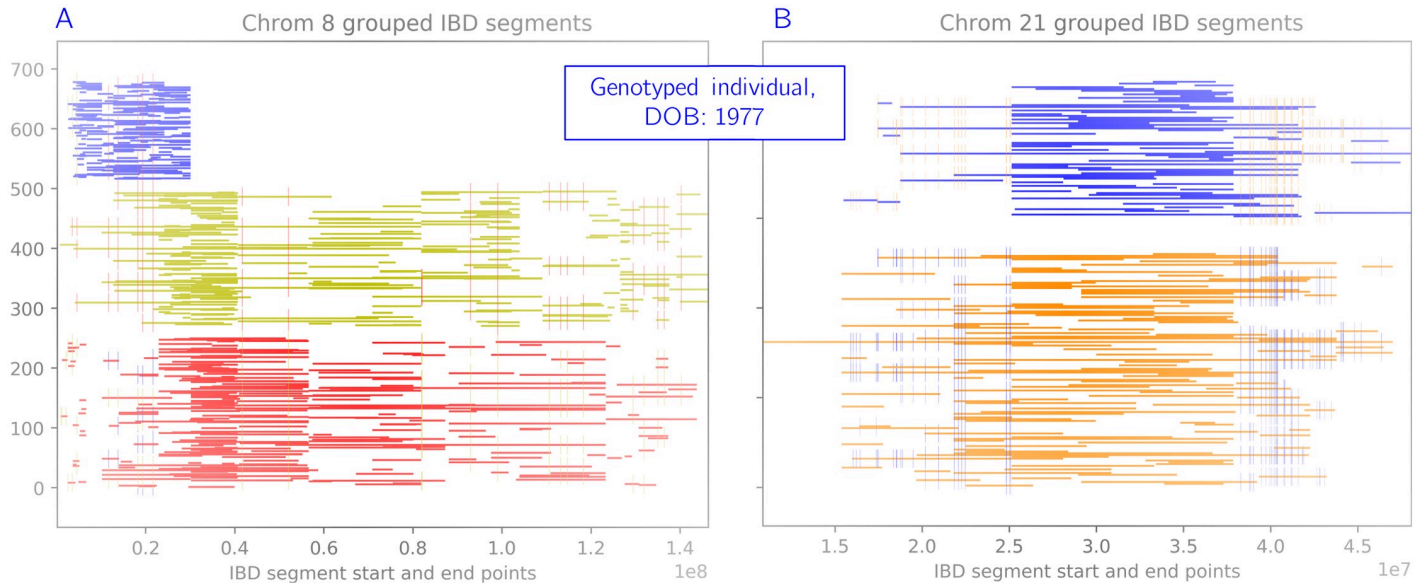


**Fig 7. Example of the grouping algorithm on a genotyped individual.** Each horizontal line represents one IBD segment shared with a cohort of other genotyped individuals. IBD segments of the same color represent haplotypes, and have a consistent sequence along the chromosome. Small vertical lines represent heterozygous sites between the two haplotypes. (A) Chrom 8: very occasionally we merge groups incorrectly and obtain three groups. (B) Chrom 21: we almost always see two clear groups (here we also see a large stretch of homozygosity).

<https://doi.org/10.1371/journal.pcbi.1008638.g007>

analysis to genotyped individuals with at least one genotyped descendant, which left 89/394 individuals. On average, these individuals had 9.87 genotyped descendants (min 1, max 48). Table 2 shows the results of this procedure for chromosomes 18–22. For example, in the case of chromosome 18 we reconstructed 71/89 individuals, with an average sequence similarity of 96.7% (measured against the corresponding true sequences). To be *reconstructed*, at least half the chromosome must be assembled for each haplotype, with sufficient support in terms of coverage and number of IBD segments (further details in **Definitions 1–2**). It is likely that we reconstructed parts of the remaining 18 individuals, but they did not meet our definition of reconstructed.

We also explored the relationship between number of genotyped descendants  $D_g$  and the probability of being reconstructed. We computed  $P(\text{reconstructed}|D_g)$ , where  $D_g$  was *low*, *medium*, and *high* based on breaks in the distribution of number of genotyped descendants. We did not find a strong relationship, perhaps because the chance of being reconstructed depends more on the pedigree structure itself and the likelihood that a particular individual can be identified as the source of an IBD segment. To address this hypothesis, we computed the Jaccard similarity coefficients between each pair of chromosomes (from 18–22). For this analysis we considered the data for each chromosome as a binary vector of length 89, with each individual being reconstructed or not. Overall the Jaccard coefficients were high (all pairs between 0.66 and 0.87, with an average of 0.79), indicating that an individual's position in the

**Table 2. Leave-one-out results.** For each chromosome 18–22, we left out one genotyped individual in turn and attempted to reconstruct their haplotypes. The second row shows how many individuals (out of 89) met our criteria for reconstructed. The third row shows the average sequence identity of the individuals we were able to reconstruct, measured against their true sequences.

	chr18	chr19	chr20	chr21	chr22
# reconstructed	71	67	57	66	67
average sequence identity	0.954	0.958	0.960	0.966	0.956

<https://doi.org/10.1371/journal.pcbi.1008638.t002>



pedigree structure is an important factor when considering our ability to reconstruct their genome.

### Simulation results

After running `thread` on the entire genome for the simulated data described above, we assessed the accuracy by comparing the reconstructed genomes to the correct simulated ones. The average accuracy of the reconstructions is shown in [Table 3](#). We note that although we simulated a small population with marriage between close relatives, the number of unique IBD segments per chromosome is less than half the observed number of unique IBD segments in the genotyped Amish individuals, which likely led to fewer reconstructed individuals.

Individual level results are shown in [Fig 8](#). Here we plotted two reconstruction metrics that increase as reconstruction is more successful—the number of chromosomes reconstructed and the average accuracy of the reconstructed chromosomes. The strongest relationship appears with generation, where more recent individuals generally have more accurate genome reconstructions ( $r = 0.61$ ). There is a mixed relationship with the number of genotyped direct descendants (children and grandchildren). Individuals with more genotyped direct descendants generally have more accurate reconstructions ( $r = 0.59$ ), but not necessarily more chromosomes reconstructed ( $r = 0.29$ ). As inbreeding coefficient increases we see a general increase in accuracy ( $r = 0.48$ ), but again not a strong relationship. We also show the relationship between generation, reconstruction accuracy, and number of chromosomes

**Table 3. Whole-genome ancestral reconstruction results: Simulated data.** The second column shows the total number of IBD pairs identified between genotyped individuals. The third column shows the number of unique IBD segments per chromosome. The fourth column shows how many iterations the algorithm needed to converge. The fifth column shows the number of ancestral (ungenotyped) individuals we were able to successfully reconstruct. The sixth column shows the average sequence similarity of the individuals we were able to reconstruct, as compared to their true genomes. The rightmost two columns show the number of individuals that we *predicted* would be very well reconstructed, along with their average accuracies.

chr	IBD pairs	unique IBDs	iter	recon.	acc. %	filter	filter acc. %
1	312526	10447	8	181	86.05	34	90.19
2	314518	9588	9	173	86.14	40	89.42
3	273032	8006	6	162	86.52	33	91.39
4	186735	7336	5	164	86.42	42	89.95
5	258649	7891	9	195	86.22	30	90.25
6	225494	7249	8	189	85.97	45	89.94
7	198285	6657	6	172	85.81	37	89.97
8	169540	5833	8	143	86.64	29	92.55
9	188457	5687	5	127	85.31	28	91.15
10	209888	6191	6	146	87.97	33	92.16
11	183196	5910	5	163	87.25	31	91.50
12	212065	6040	5	168	86.22	37	89.12
13	136549	4561	7	156	86.62	28	91.19
14	121796	3858	6	132	86.63	29	91.96
15	157815	4837	5	169	87.52	27	92.86
16	150385	4515	6	134	88.34	29	92.70
17	136973	4351	6	148	87.34	30	90.65
18	112425	3885	7	158	86.74	28	90.54
19	120179	3523	4	125	86.82	23	88.61
20	135525	3959	5	143	87.40	23	90.52
21	79550	2109	6	90	88.73	17	92.96
22	86547	2528	4	85	86.90	17	90.27

<https://doi.org/10.1371/journal.pcbi.1008638.t003>

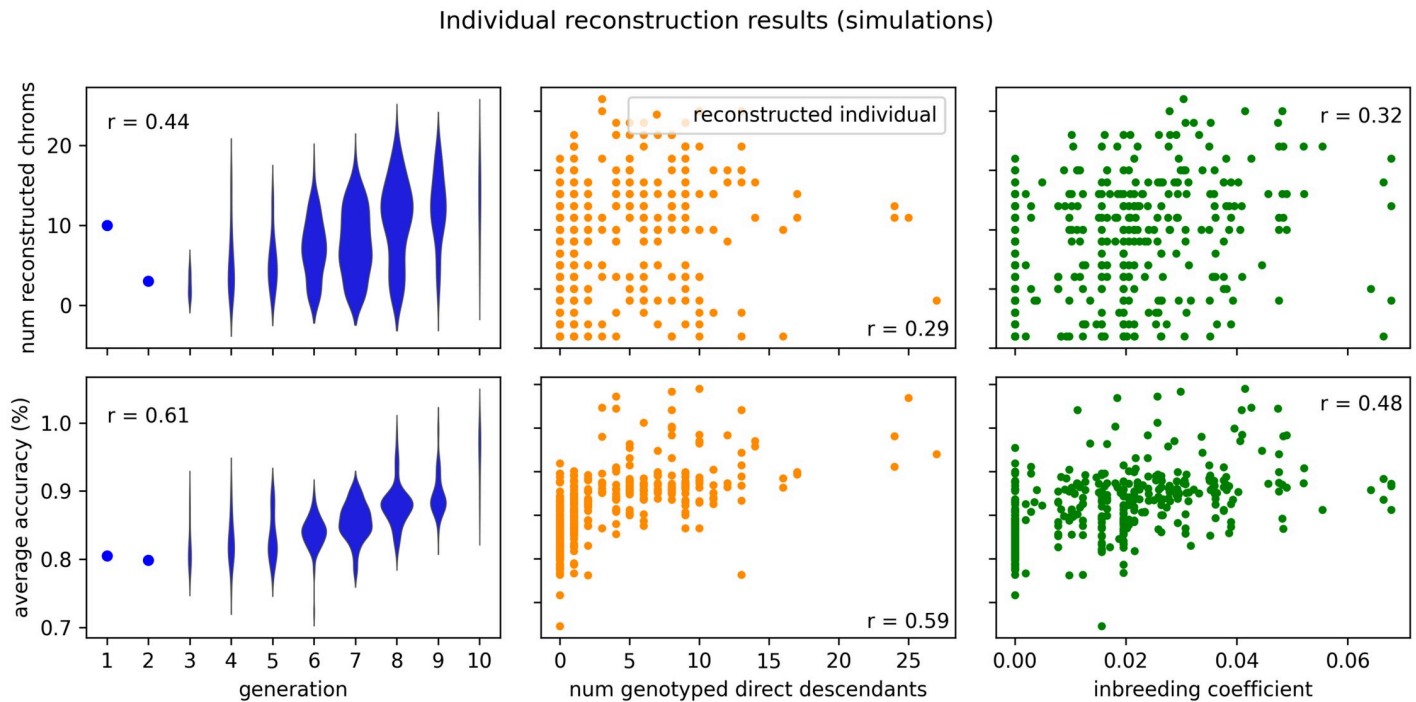


**Fig 8. Individual results: Simulated data.** The same results as Table 3, but shown on the individual level. The top set of figures shows reconstruction completeness as measured by the number of reconstructed chromosomes. The bottom set of figures shows reconstruction accuracy as measured by sequence identity averaged over the reconstructed chromosomes. These two metrics are plotted against three statistics about each individual: the generation number (lower is more ancient), the number of genotyped direct descendants (children and grandchildren), and the inbreeding coefficient as calculated by PedHunter using the entire AGDB comprised of more than 500,000 individuals. Correlation coefficients are shown for each relationship.

<https://doi.org/10.1371/journal.pcbi.1008638.g008>

reconstructed in a more holistic fashion in S3 Fig. In addition, we demonstrate a few examples of how IBD segments are removed during conflict resolution in S4 Fig. In the first example we show how incorrectly placed IBD segments were successfully identified and removed, leading to a perfect reconstruction. In the second case we show an example where `thread` failed to identify incorrect segments, leading to a reduced reconstruction accuracy.

The results of varying pre-migration population size and IBD source selection algorithms for chromosome 21 are shown in Fig 9. The greedy algorithm is denoted “min path” and the probabilistic algorithm is denoted “max prob”. As the population size increases, we generally see more accurate reconstructions, but fewer individuals reconstructed. This tradeoff is likely due in part to differences in cohort size—if only a few individuals share an IBD segment, its source can be more easily identified than if many individuals share the IBD. This leads to more accurate reconstructions, but fewer individuals will be assigned sufficient IBD segments. The probabilistic source identification algorithm typically results in fewer reconstructed individuals, but higher accuracies (up to 98.38%). By definition the “max prob” source will have at least as many paths as the “min path” source, but there will be fewer individuals on all paths from the source to the cohort. This leads to fewer IBD segments placed into individuals, but higher accuracy for those that are placed. In terms of runtime, “min path” is usually slightly longer. The average runtime for the experiments in Fig 9 was 19.8 minutes for “min path” and 16.7 minutes for “max prob”.

In S5 Fig we sort the individuals reconstructed by “min path” and “max prob” by generation (for pre-migration population size 400). We observe that individuals well-reconstructed by “min path” are also often well-reconstructed by “max prob”, especially in the most recent

## Reconstruction results as founder population size increases

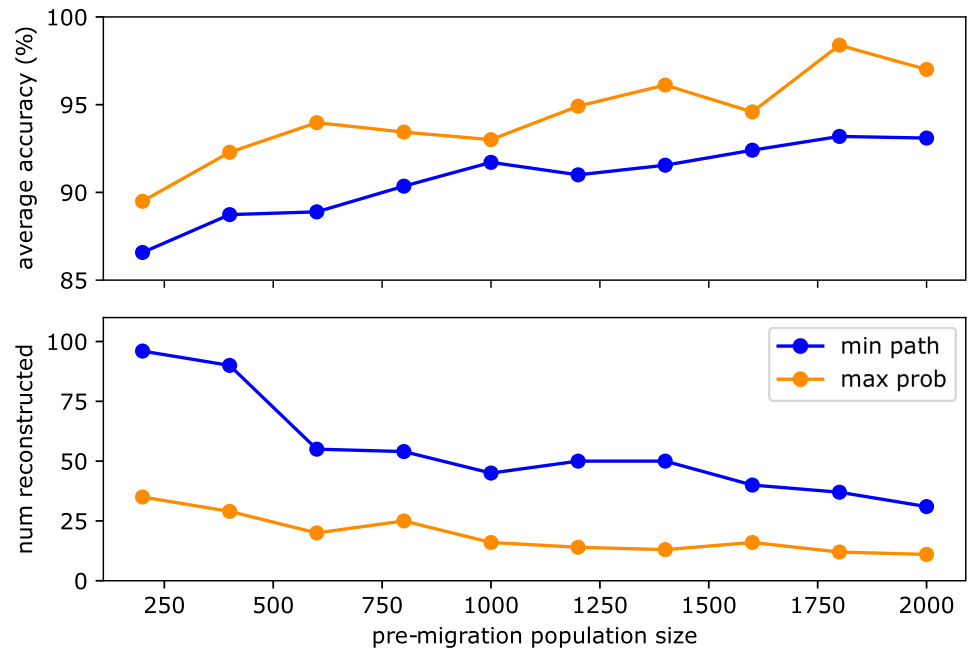


**Fig 9. Varying population size and source-finding approach: Simulated data.** The top panel shows the average reconstruction accuracy of chromosome 21 as a function of pre-migration population size. The bottom panel shows the number of reconstructed individuals for the corresponding scenarios. The greedy source-identification algorithm is denoted “min path” and the probabilistic algorithm is denoted “max prob”. There is a clear tradeoff between accuracy and the number of individuals reconstructed.

<https://doi.org/10.1371/journal.pcbi.1008638.g009>

generations. “Max prob” does not typically reconstruct individuals that have low accuracy in “min path”. As the generations become more ancient, “max prob” reconstructs several individuals very accurately (e.g. in generation 5) that are not reconstructed at all by “min path”. This corroborates the idea that when “min path” and “max prob” choose different sources for an IBD segment, “max prob” will typically choose a more ancient source, enabling the accurate reconstruction of some ancient individuals.

The results of using the true IBD segments from *Ped-sim* are shown in [S1 Table](#), for chromosomes 18–22. Overall there were more unique IBD segments than called by *GERMLINE*, possibly due to more accurate detection of the endpoints of IBD segments. Overall however, the results do not show dramatic improvement, and the number of reconstructed individuals is typically fewer than when using *GERMLINE* (but not less accurate). This indicates that IBS called as IBD is not likely a major cause of inaccuracies in *thread* reconstructions. (For IBS segments with large cohort sizes, if no sources can be identified then we skip the segment.) Based on the results in [Fig 9](#), source confusion likely plays a bigger role in creating reconstruction error.

Finally, the results of modifying the strong group criteria are shown in [S1 Table](#), for chromosomes 18–22. Setting A reduces the number of reconstructed individuals, which makes sense since it is a strictly stronger criteria than before. But gains in accuracy are minimal. Setting B produces similar results as the original settings, indicating that much more relaxed criteria are needed to reconstruct individuals in more ancient generations (which would likely lead

to decreases in reconstruction completeness and accuracy). Overall, ancient individuals remain difficult to reconstruct.

### Reconstruction results

After running `thread` on each chromosome using the entire Amish pedigree and all genotyped individuals, we assessed the results in terms of how many individuals were successfully reconstructed. For all chromosomes, `thread` converged in 5-10 iterations, and the number of successfully reconstructed ancestral individuals ranged between 162 and 248 (24%-36% of the 686 individuals with genotyped descendants). On average this is 224 individuals per chromosome, with an overall average of 79% of their haplotypes reconstructed. See [Table 4](#) for the details of each chromosome. Using a single CPU, the runtime was always less than 24 hours for a single chromosome. Typical memory requirements were 40G for all but the largest few chromosomes, which needed 80G.

We also compared the IBD length distributions of the simulated data and the real data, as shown in [Fig 10](#). In general the simulations have fewer unique IBDs (especially short IBDs), but the distribution shapes are similar.

The conflict resolution step was essential for removing misplaced IBD segments and routing them to other sources. An example is shown in [Fig 11](#). In this case, the green and blue groups were removed from this individual, as they were much less *strong* than the cyan and red groups. In the next iteration, we re-source the associated IBDs and consider the individual reconstructed. Examples of successful ancestral reconstructions are shown in [Fig 12](#), for a

**Table 4. Whole-genome ancestral reconstruction results: Amish data.** The second column shows the total number of IBD pairs identified between genotyped individuals. The third column shows the number of unique IBD segments per chromosome. The fourth column shows how many iterations the algorithm needed to converge. The fifth column shows the number of ancestral (ungenotyped) individuals we were able to successfully reconstruct. We require a successfully reconstructed chromosome to have two haplotypes that cover at least half the chromosome, with sufficient IBD support for each haplotype. Finally, the last column shows the runtime.

chr	IBD pairs	unique IBDs	iter	reconstructed	time (hrs)
1	351230	28359	10	248	22.91
2	288059	26962	7	248	19.19
3	246909	22488	6	232	11.23
4	250878	20980	6	223	9.83
5	219746	19448	7	236	9.14
6	244751	20883	7	224	10.76
7	225155	19370	6	216	6.73
8	222422	16950	6	241	4.96
9	232309	17547	6	236	3.85
10	220391	16822	7	223	6.22
11	198145	15416	8	238	5.49
12	175552	16712	7	227	5.08
13	161721	13296	5	202	2.74
14	169906	11867	6	239	2.36
15	180198	12179	7	248	2.60
16	143985	13010	7	251	2.74
17	121688	11768	5	195	2.44
18	129719	11359	7	219	2.13
19	141857	10702	6	218	1.44
20	139179	9910	8	235	1.95
21	77745	5020	6	175	0.68
22	73766	5773	5	162	0.77

<https://doi.org/10.1371/journal.pcbi.1008638.t004>

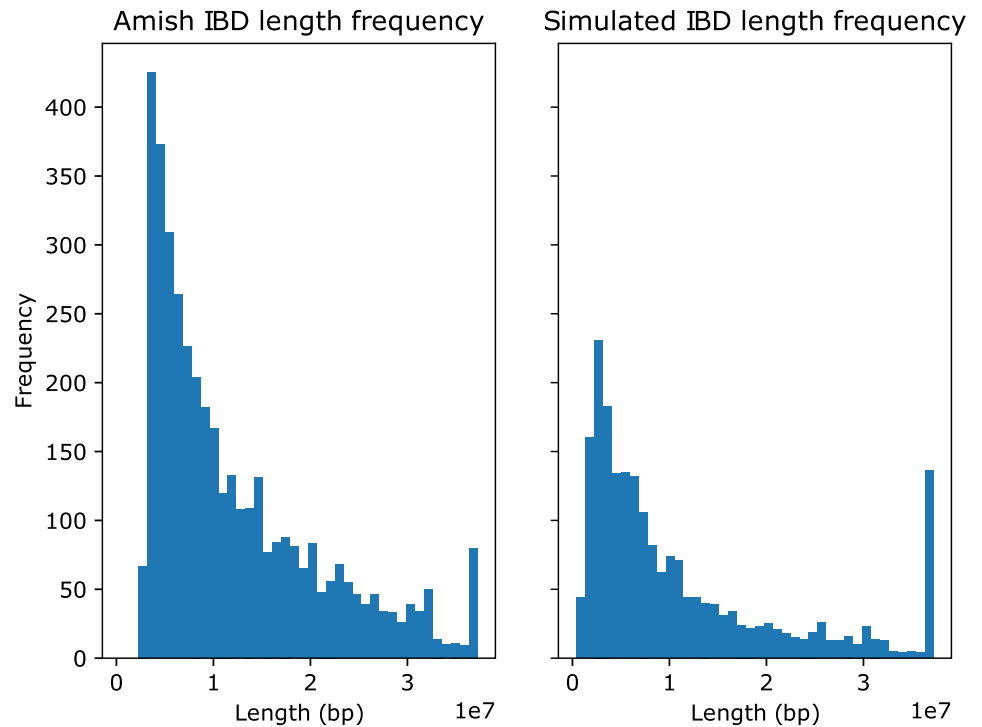


**Fig 10. IBD length distribution.** Left: IBD length distribution for the real data for chromosome 21. Right: IBD length distribution for the simulated data for chromosome 21. x-axis units are 10Mbp.

<https://doi.org/10.1371/journal.pcbi.1008638.g010>

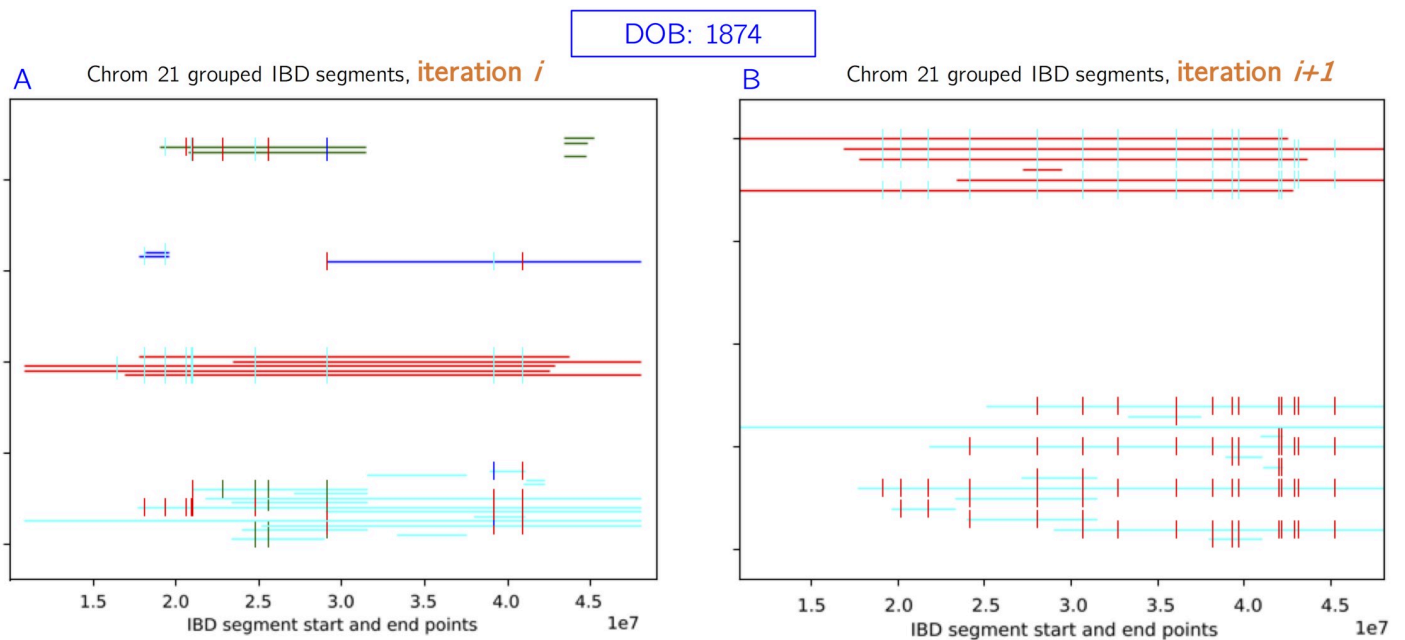


**Fig 11. Conflict resolution example.** The blue and green groups are removed, since they are less *strong* than the cyan and red groups. In the next iteration, we retain only strong groups and consider the individual reconstructed. Newly sourced IBDs after this point may not conflict with these reconstructed haplotypes.

<https://doi.org/10.1371/journal.pcbi.1008638.g011>

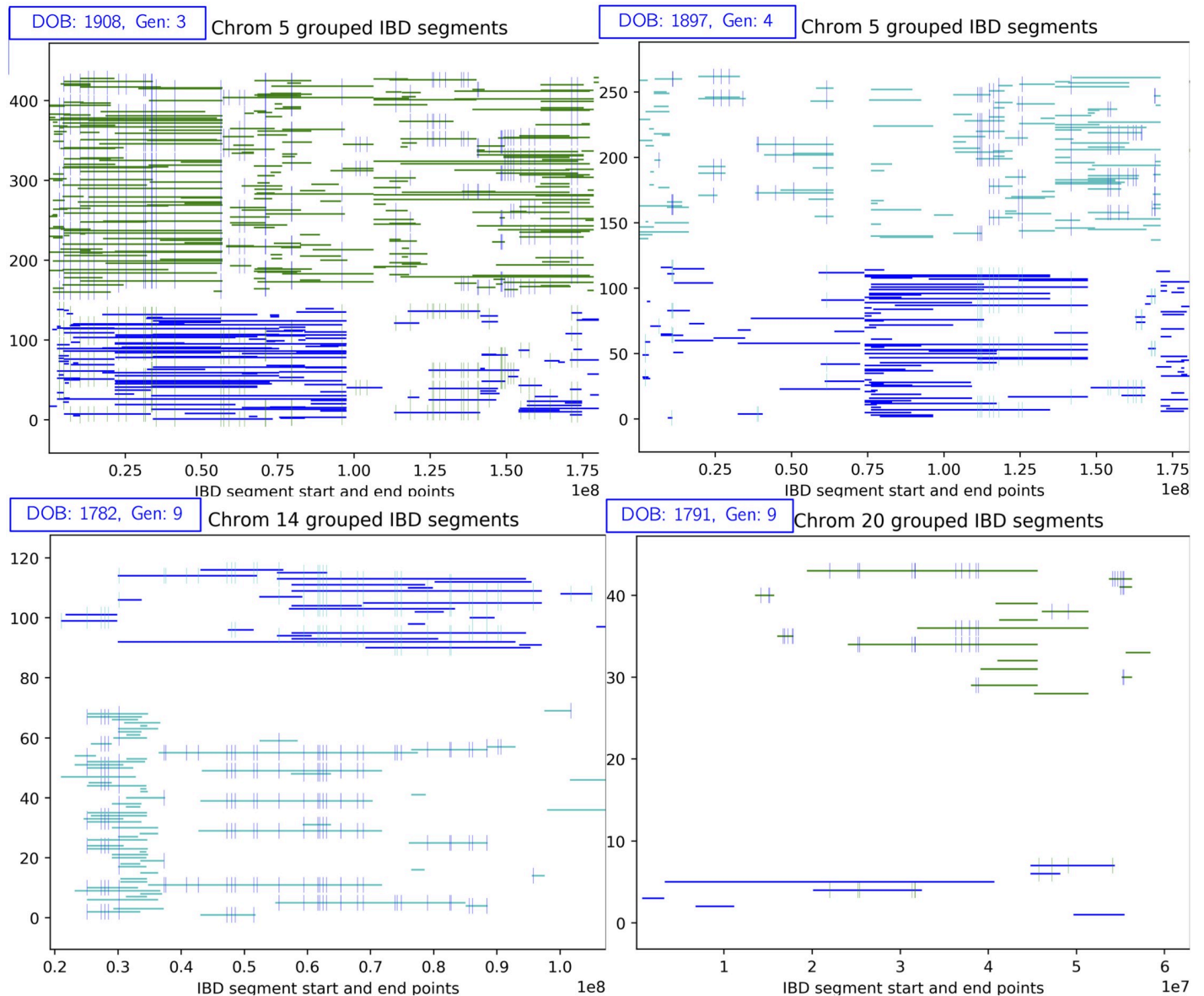


**Fig 12. Successful ancestral reconstructions.** Ancestral reconstructions of ungenotyped individuals, from a variety of chromosomes and generations (back in time). As we go back in time, we generally have fewer IBD segments to group.

<https://doi.org/10.1371/journal.pcbi.1008638.g012>

variety of different chromosomes and generations back in time. As expected, in the more distant generations, we place fewer IBD segments and generally have less coverage over the chromosome.

Although we reconstruct many individuals well in the recent generations, there are many haplotypes we are unable to resolve. Several examples are shown in S6 Fig. Sometimes `thread` constructs one haplotype successfully, but not the other (S6A Fig). Often we have some successful reconstruction, but the groups do not meet our threshold for “two strong” since the third group has too many IBD segments (S6B Fig). Sometimes there are four groups, which could represent ambiguity between the individual’s spouse or close relative (S6C Fig).



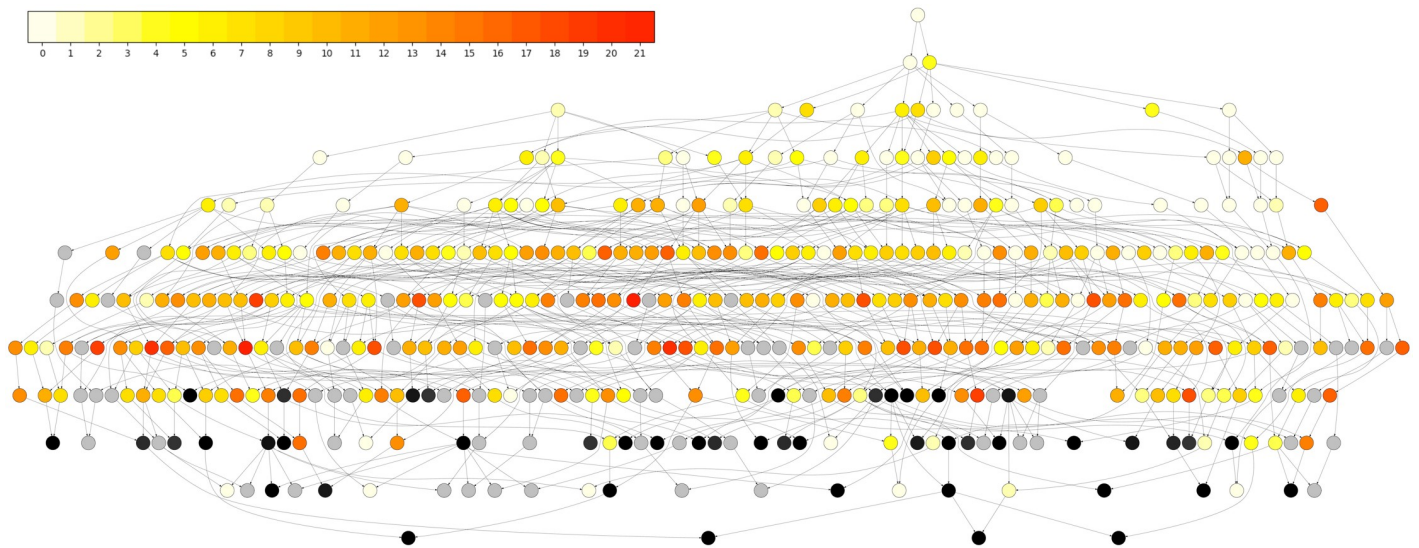


**Fig 13. Nuclear family graph.** Each node represents a nuclear family (parents and children). When a child of one family becomes the parent of another, we draw an edge. Black nodes have at least 80% of the family genotyped. Gray nodes have at least 80% of the family without genotyped descendants. Yellow (fewer)—Red (more) colors represent the average number of chromosomes reconstructed for the individuals in the family.

<https://doi.org/10.1371/journal.pcbi.1008638.g013>

Sometimes there are too many IBD segments placed within an individual, which could arise if they have many descendants (S6D Fig).

Table 4 and Fig 13 show our results in a holistic view. Table 4 shows how many individuals we are successfully reconstructing for each chromosome. Fig 13 shows these same results on the family level, broadly indicating which individuals we are reconstructing well. S7 Fig shows these results on the individual level.

### Lost regions

We were particularly interested in regions of the genome that have been “lost” over time, as they may be deleterious. To assess this, we looked for regions of the genome with a low fraction of reconstructed individuals. We measured this by analyzing non-overlapping sliding windows of 50 SNPs; if less than 40% of the bases in a window were not reconstructed, we declared the region difficult to reconstruct. We then merged adjacent regions to form a set of “lost” regions. The telomeres of each chromosome formed the majority of regions that were difficult to reconstruct, which is expected. Across the entire genome, there was only one non-telomeric region that met our criteria for a lost region, chr16:70824983-71066078. This region on chromosome band 16q22, containing most of the large gene *HYDIN* (chr16:70835987-71264625), is known to be genomically unstable in two ways that could make it difficult to reconstruct haplotypes. The more likely difficulty is that there are frequent segmental duplications with varying breakpoints in this region [54], which have been associated with autism [55].

Re-examination of the copy-number variants (CNVs) called in a previous study [56] by RLK using the software PennCNV [57] shows that there are overlapping intervals of a duplication within the interval chr16:70696689-70745016 in 67 genotyped individuals in the pedigree. One boundary of the CNV is shared by most of the 67 individuals. The other boundary, however, varies considerably, which is unusual for an inherited CNV and may reflect either the difficulty in calling genotypes mentioned above or genomic instability. The average length of the duplication among the 67 individuals is 32,641 bp.

The less likely difficulty is that in evolution, the instability of this region led to a recent (by evolutionary time scales) paralogous duplication of the region that landed on human chromosome band 1q21, and contains the paralogous gene *HYDIN2*. The chromosome 1 copy is sufficiently similar to the 16q22 that it caused difficulty in assembling early versions of the human genome [58]. The sequence similarity of the 16q22 and 1q21 segments could lead to imperfect genotypes in either interval.

## Discussion

The methodology behind `thread` represents a new direction for ancestral reconstruction that scales in both the number of individuals and the number of loci. Previous ancestral haplotype reconstruction algorithms have either been too slow to apply, too rigid to accommodate a complex pedigree, perform steps by hand, or consider a more diverse ancestral population. Although a likelihood approach to reconstruction is theoretically possible, our work represents a practical alternative as pedigree size and complexity continues to grow. We note that our method is most suitable when genotyped individuals exhibit high levels of IBD sharing, ideally with each IBD segment descending from a single ancestor. `thread` may need further development to handle pedigrees from populations with very large effective population sizes and/or high levels of admixture.

Through simulations we validate `thread` in a variety of scenarios, including a range of ancestral population sizes. With realistic simulation parameters it was difficult to obtain the number of unique IBDs found in the Amish population, which is likely a reason why we reconstruct fewer individuals in simulations. One overall trend is that as the population size increases, we reconstruct fewer individuals, but their reconstructions are more accurate. Well reconstructed individuals also tend to be closer to the present. A future version of the algorithm could use these observations to build up reconstructions gradually—after an initial group of individuals is accurately reconstructed, they could be added to the original list of “genotyped” individuals, then the entire algorithm could be run again to reconstruct a next group of individuals, and so on. This type of approach might be particularly useful for populations with less endogamy, where reconstructing ancient individuals is naturally more difficult.

There are many possible algorithmic improvements to the IBD-based approach of `thread`. The grouping algorithm could make use of the genetic map to merge groups at recombination hotspots. More realistic simulations could model crossover interference and sex-specific recombination maps, as in [53]. In rare cases (only chromosome 21 for one genotyped individual) the entire chromosome is homozygous, so the criteria of two strong groups could be relaxed or made more flexible. As there is a tradeoff between accuracy and number of individuals reconstructed for the “min path” and “max prob” algorithms, these two strategies could be merged.

In terms of implementation, `thread` could be parallelized across IBD segments and individuals. Simulations and runtime profiling suggest that for the Amish pedigree, the bottleneck is the implementation of the conflict resolution procedures inside Algorithm 1. If the conflict resolution were faster, this would enable more complicated conflict resolution strategies, which may improve reconstruction accuracy. The running time analysis shows that for animal pedigrees with more generations, the source and descendance path finding (Algorithm 2) will be the bottleneck because it takes exponential time in the number of generations (in the worst case).

An important use case for genealogies of isolated populations has been to study rare recessive diseases, including finding causative genes. After collecting data on living affected individuals, it may be of interest to find the most likely paths of inheritance of the rare

disease-causing allele, which is a simpler problem than assigning (not necessarily rare) haplotypes across the genome. In AGDB and the associated software `PedHunter`, the problem of finding the best paths of inheritance to explain the presence of a rare allele is solved as a combinatorial optimization problem closely related to the classical minimum Steiner tree problem in graphs [59] and large instances can be solved to optimality using mixed integer linear programming (e.g., [60]) even though the Steiner tree problem is NP-complete. In the BALSAC <http://balsac.uqac.ca/> project that contains a large genealogy of the population of Québec, the rare allele inheritance problem is formulated statistically and is solved in the software `ISGen` (<https://github.com/DomNelson/ISGen>) using Monte Carlo Markov Chain techniques [61] extending earlier seminal work of Geyer and Thompson on a Hutterite genealogy [62]. For the haplotype problem, the methods in `thread` are based on deterministic combinatorial algorithms, like the methods in `PedHunter`. One could imagine instead solving the haplotype assignment problem by MCMC methods.

The most major consideration for the utility of `thread` is data availability. On one hand, collection of human genealogies is increasing due to popular interest in genealogy research. One example that has been used in medical genetics studies is the historical genealogy collected by deCODE Genetics of more than 630,000 people who lived in Iceland over many generations [63]; in comparison, AGDB contains approximately 540,000 individuals. There are also large animal pedigrees for which `thread` may be suitable. On the other hand, the popularity of SNP genotyping is declining as the cost of DNA sequencing declines and because SNP arrays based on variants seen in HapMap Populations are not ideal to study populations such as the Amish [64]. Whole-genome sequencing (WGS) would reveal genotypes genome-wide, but at present, the less expensive whole exome sequencing (WES) is used more than WGS because most disease-relevant mutations are thought to be in exomes. WES reveals SNPs and their genotypes in any regions that are covered by the exome kit being used, but the placement of genes and their exons across the human genome is far from uniform. Thus, the potential application of `thread` to complex pedigrees will increase as the cost of WGS decreases further.

Individual-level reconstruction opens the door for many types of downstream analysis. Using reconstructed genomes to augment GWAS could increase sample sizes by hundreds of individuals when the phenotype is known. More generally, quantifying allele frequency changes, transmission distortion, and un-reconstructable (“lost”) regions allows us to model genome dynamics on a recent time scale. `thread` could be applied to other genetically characterized endogamous populations with high levels of recessive traits, such as Mennonites and Hutterites [65]. Our method would also be suitable for model organisms and domestic animals, where extensive pedigree records are common.

In addition, our results could be used to find individuals of clinical significance in cases where a gene-inhibiting drug may provide a therapeutic option for a disease. More specifically, loss of function (LoF) mutations in some genes have shown to protect against disease [66, 67]. If a loss of function allele has been observed, then haplotype reconstruction in any large pedigree makes it possible to identify carriers. If in addition, the pedigree has one or more loops, then haplotype reconstruction makes it possible to identify extremely rare individuals who may be homozygous for the LoF allele.

## Conclusion

In this work, we gave a formal algorithmic treatment of the problem of reconstructing ancestral haplotypes from the genotypes of individuals in the most recent generations of an extended pedigree. In publicly available software called `thread`, we designed and

implemented a new algorithm for ancestral haplotype reconstruction that can handle highly complex pedigrees, which arise in isolated human populations and in animal breeding. We evaluated the performance of our algorithm on an Old Order Amish pedigree of 1338 individuals, many of whom have been diagnosed with bipolar or other mood disorders. Versions of this pedigree have been studied in psychiatric and statistical genetics for decades, as the genetic variations contributing to bipolar disorder remain poorly understood. Using our new algorithm, it is possible to trace the inheritance of many haplotypes in this pedigree, including those of long-deceased individuals. In future clinical studies, this should lead to a better understanding of which haplotypes are associated with bipolar disorder in this Amish pedigree. We anticipate that `thread` could be similarly useful in other endogamous populations.

## Supporting information

**S1 Fig. Pedigree structure: 1338 individuals over 10 generations.** Squares represent males and circles represent females. Dotted lines connect the same individual appearing in two different parts of the pedigree. Filled in symbols represent genotyped individuals.

(EPS)

**S2 Fig. Inbreeding coefficients for each individual in the pedigree structure from S1 Fig.**

Inbreeding coefficients were computed using the software `PedHunter` and the entire AGDB.

(EPS)

**S3 Fig. Simulation results per individual.** The generation of the individual is plotted on the  $x$ -axis (higher number generations are more recent). For the chromosomes we were able to reconstruct, we compute and plot the accuracy on the  $y$ -axis. Symbol size and color shows how many chromosomes we were able to reconstruct.

(EPS)

**S4 Fig. Demonstration of removed segments in simulations.** Headers for each set of figures show the individual ID and overall reconstruction accuracy for chromosome 21. Each horizontal line represents one IBD segment shared with a cohort of genotyped individuals. The top row of figures for each individual represent IBDs assigned at the beginning of each iteration. The bottom row represents the IBDs that remain after conflict resolution. Light blue segments are correct segments added during iteration 0, and dark blue segments are correct and added during iteration 1. Gray segments are incorrect. A) For this individual, we successfully removed these gray segments and achieved 100% reconstruction accuracy. B) For this individual, we failed to detect several incorrect IBD segments and achieved a lower reconstruction accuracy.

(EPS)

**S5 Fig. “Min path” vs. “max prob”: Simulated data.** On the  $x$ -axis are all individuals reconstructed by the “min path” (blue) and “max prob” (orange) source finding algorithms, for a pre-migration population size 400. The presence of both blue and orange bars on either side of a tick mark indicates the individual was reconstructed by both methods. The  $y$ -axis shows the reconstruction accuracy of each individual. The individuals are sorted by generation (more ancient to the left and more recent to the right). We observe that “max prob” reconstructs fewer individuals than “min path”, but they are generally more accurate.

(EPS)

**S6 Fig. Unsuccessful reconstruction examples.** Each horizontal line represents one IBD segment shared with a cohort of other genotyped individuals. IBD segments of the same color represent haplotypes, and have a consistent sequence along the chromosome. Small vertical

lines represent heterozygous sites between the two haplotypes. A) Occasionally we only build one haplotype (which may not actually be unsuccessful if the individual was entirely homozygous for the given chromosome). B) Sometimes we have a fairly strong reconstruction, but due to the presence of other groups it does not meet our threshold for two strong group. C) Four groups may indicate ambiguity with a spouse or other close relative. D) Sometimes we see many groups and cannot resolve the individual.

(EPS)

**S7 Fig. Position of reconstructed individuals in the pedigree.** Black: genotyped individual, white: no genotyped descendants, yellow-red heatmap: represents number of chromosomes reconstructed, blue: no chromosomes reconstructed.

(EPS)

**S1 Table. Algorithm experimentation: Simulated data.** The first block of results shows the output of `thread` when run on the true IBD segments from `Ped-sim`. The second block of results shows setting A of the strong groups criteria, which requires more IBD support for individuals in ancient generations (described in more detail the main text). Similarly, the third block of results shows setting B, which requires more IBD support but relaxes the length requirements for older generations. The third column shows the number of unique IBDs (called by `GERMLINE` in the second two blocks). The fourth column shows how many iterations the algorithm needed to converge. The fifth column shows the number of ancestral (ungenotyped) individuals we were able to successfully reconstruct. The last column shows the average sequence similarity of the individuals we were able to reconstruct, as compared to their true genomes.

(XLSX)

**S1 Text. Algorithm pseudocode, complexity analysis, and probabilistic source identification.** Here we include the technical details of `thread`. Algorithm 1: overview of `thread`. Algorithm 2: source and descendance path finding. Algorithm 3: grouping IBD segments within individuals. Then we specify the time complexity of `thread`, and finally we include the mathematical details of the probabilistic source finding algorithm.

(PDF)

## Acknowledgments

The authors would like to thank Jeff Knerr and Joe Cammisa for providing invaluable computational support, Amy Williams for guidance with simulations, Iain Mathieson for feedback on the method and manuscript, and the participants in the Amish Study of Major Affective Disorder (ASMAD).

## Author Contributions

**Conceptualization:** Rachel L. Kember, Maja Bućan, Sara Mathieson.

**Data curation:** Alejandro A. Schäffer, Rachel L. Kember.

**Formal analysis:** Kelly Finke, Michael Kourakos, Gabriela Brown, Huyen Trang Dang, Shi Jie Samuel Tan, Sara Mathieson.

**Methodology:** Kelly Finke, Michael Kourakos, Gabriela Brown, Yuval B. Simons, Alejandro A. Schäffer, Rachel L. Kember, Maja Bućan, Sara Mathieson.

**Resources:** Shweta Ramdas, Alejandro A. Schäffer.



**Software:** Kelly Finke, Michael Kourakos, Gabriela Brown, Huyen Trang Dang, Shi Jie Samuel Tan, Sara Mathieson.

**Supervision:** Maja Bućan, Sara Mathieson.

**Validation:** Huyen Trang Dang, Shi Jie Samuel Tan, Yuval B. Simons, Alejandro A. Schäffer, Sara Mathieson.

**Visualization:** Kelly Finke, Sara Mathieson.

**Writing – original draft:** Kelly Finke, Sara Mathieson.

**Writing – review & editing:** Kelly Finke, Gabriela Brown, Yuval B. Simons, Alejandro A. Schäffer, Rachel L. Kember, Maja Bućan, Sara Mathieson.

## References

1. Campbell CD, Chong JX, Malig M, Ko A, Dumont BL, Han L, et al. Estimating the human mutation rate using autozygosity in a founder population. *Nature Genetics*. 2012; 44(11):1277–1281. <https://doi.org/10.1038/ng.2418> PMID: 23001126
2. Sun JX, Helgason A, Masson G, Ebenesersdóttir SS, Li H, Mallick S, et al. A direct characterization of human mutation based on microsatellites. *Nature Genetics*. 2012; 44(10):1161–1165. <https://doi.org/10.1038/ng.2398> PMID: 22922873
3. Broman KW, Murray JC, Sheffield VC, White RL, Weber JL. Comprehensive human genetic maps: individual and sex-specific variation in recombination. *American Journal of Human Genetics*. 1998; 63(3):861–869. <https://doi.org/10.1086/302011> PMID: 9718341
4. Kong A, Gudbjartsson DF, Sainz J, Jonsson GM, Gudjonsson SA, Richardsson B, et al. A high-resolution recombination map of the human genome. *Nature Genetics*. 2002; 31(3):241–247. <https://doi.org/10.1038/ng917> PMID: 12053178
5. Keightley PD, Ness RW, Halligan DL, Haddrill PR. Estimation of the spontaneous mutation rate per nucleotide site in a *Drosophila melanogaster* full-sib family. *Genetics*. 2014; 196(1):313–320. <https://doi.org/10.1534/genetics.113.158758> PMID: 24214343
6. Tatsumoto S, Go Y, Fukuta K, Noguchi H, Hayakawa T, Tomonaga M, et al. Direct estimation of de novo mutation rates in a chimpanzee parent-offspring trio by ultra-deep whole genome sequencing. *Scientific Reports*. 2017; 7(1):13561. <https://doi.org/10.1038/s41598-017-13919-7> PMID: 29093469
7. Smeds L, Mugal CF, Qvarnström A, Ellegren H. High-resolution mapping of crossover and non-crossover recombination events by whole-genome re-sequencing of an avian pedigree. *PLoS Genetics*. 2016; 12(5):e1006044. <https://doi.org/10.1371/journal.pgen.1006044> PMID: 27219623
8. McParland S, Kearney J, Rath M, Berry D. Inbreeding trends and pedigree analysis of Irish dairy and beef cattle populations. *Journal of Animal Science*. 2007; 85(2):322–331. <https://doi.org/10.2527/jas.2006-367> PMID: 17040944
9. Chen N, Juric I, Cosgrove EJ, Bowman R, Fitzpatrick JW, Schoech SJ, et al. Allele frequency dynamics in a pedigreed natural population. *PNAS*. 2019; 116(6):2158–2164. <https://doi.org/10.1073/pnas.1813852116> PMID: 30598449
10. Beaty T, Kwiterovich P Jr, Khoury M, White S, Bachorik P, Smith H, et al. Genetic analysis of plasma sitosterol, apoprotein B, and lipoproteins in a large Amish pedigree with sitosterolemia. *American Journal of Human Genetics*. 1986; 38(4):492–504. PMID: 3706300
11. Peltonen L, Palotie A, Lange K. Use of population isolates for mapping complex traits. *Nature Reviews Genetics*. 2000; 1:182–190. <https://doi.org/10.1038/35042049> PMID: 11252747
12. Locke AE, Steinberg KM, Chiang CWK, Service SK, Havulinna AS, Stell L, et al. Exome sequencing of Finnish isolates enhances rare-variant association power. *Nature*. 2019; 572:323–328. <https://doi.org/10.1038/s41586-019-1457-z> PMID: 31367044
13. Sveinbjörnsdóttir S, Hicks AA, Jonsson T, Pétursson H, Guðmundsson G, Frigge ML, et al. Familial aggregation of Parkinson's disease in Iceland. *New England Journal of Medicine*. 2000; 343(24):1765–1770. <https://doi.org/10.1056/NEJM200012143432404> PMID: 11114315
14. Grant SF, Thorleifsson G, Frigge ML, Thorsteinsson J, Gunnlaugsdóttir B, Geirsson ÁJ, et al. The inheritance of rheumatoid arthritis in Iceland. *Arthritis & Rheumatism*. 2001; 44(10):2247–2254. [https://doi.org/10.1002/1529-0131\(200110\)44:10%3C2247::AID-ART387%3E3.0.CO;2-Y](https://doi.org/10.1002/1529-0131(200110)44:10%3C2247::AID-ART387%3E3.0.CO;2-Y) PMID: 11665965
15. Torkamani A, Wineinger NE, Topol EJ. The personal and clinical utility of polygenic risk scores. *Nature Reviews Genetics*. 2018; 19:581–590. <https://doi.org/10.1038/s41576-018-0018-x> PMID: 29789686



16. Kember RL, Hou L, Ji X, Andersen LH, Ghorai A, Estrella LN, et al. Genetic pleiotropy between mood disorders, metabolic, and endocrine traits in a multigenerational pedigree. *Translational Psychiatry*. 2018; 8(218):1–12.
17. de Villena FPM, Sapienza C. Nonrandom segregation during meiosis: the unfairness of females. *Mammalian Genome*. 2001; 12(5):331–339. <https://doi.org/10.1007/s003350040003>
18. Meyer WK, Arbeithuber B, Ober C, Ebner T, Tiemann-Boege I, Hudson RR, et al. Evaluating the evidence for transmission distortion in human pedigrees. *Genetics*. 2012; 191(1):215–232. <https://doi.org/10.1534/genetics.112.139576> PMID: 22377632
19. Hayes BJ, Lewin HA, Goddard ME. The future of livestock breeding: genomic selection for efficiency, reduced emissions intensity, and adaptation. *Trends in Genetics*. 2013; 29(4):206–214. <https://doi.org/10.1016/j.tig.2012.11.009> PMID: 23261029
20. Lander ES, Green P. Construction of multilocus genetic linkage maps in humans. *PNAS*. 1987; 84:2363–2367. <https://doi.org/10.1073/pnas.84.8.2363> PMID: 3470801
21. Sobel E, Lange K. Descent graphs in pedigree analysis: applications to haplotyping, location scores, and marker-sharing statistics. *American Journal of Human Genetics*. 1996; 58(6):1323–1337. PMID: 8651310
22. Abecasis GR, Cherny SS, Cookson WO, Cardon LR. Merlin—rapid analysis of dense genetic maps using sparse gene flow trees. *Nature Genetics*. 2002; 30(1):97–101. <https://doi.org/10.1038/ng786> PMID: 11731797
23. Sobel E. SimWalk2: Overview; 2004. Available from: <https://watson.hgen.pitt.edu/docs/simwalk2.html>.
24. Mott R, Talbot CJ, Turri MG, Collins AC, Flint J. A method for fine mapping quantitative trait loci in outbred animal stocks. *PNAS*. 2000; 97(23):12649–12654. <https://doi.org/10.1073/pnas.230304397> PMID: 11050180
25. Liu EY, Zhang Q, McMillan L, de Villena FPM, Wang W. Efficient genome ancestry inference in complex pedigrees with inbreeding. *Bioinformatics*. 2010; 26(12):i199–i207. <https://doi.org/10.1093/bioinformatics/btq187> PMID: 20529906
26. Zheng C, Boer MP, van Eeuwijk FA. Reconstruction of Genome Ancestry Blocks in Multiparental Populations. *Genetics*. 2015; 200:1073–1087. <https://doi.org/10.1534/genetics.115.177873> PMID: 26048018
27. Zhang K, Sun F, Zhao H. HAPLORE: a program for haplotype reconstruction in general pedigrees without recombination. *Bioinformatics*. 2004; 21(1):90–103. <https://doi.org/10.1093/bioinformatics/bth388> PMID: 15231536
28. Fishelson M, Dovgolevsky N, Geiger D. Maximum likelihood haplotyping for general pedigrees. *Human Heredity*. 2005; 59(1):41–60. <https://doi.org/10.1159/000084736> PMID: 15802921
29. Lindholm E, Åberg K, Ekholm B, Pettersson U, Adolfsson R, Jazin EE. Reconstruction of ancestral haplotypes in a 12-generation schizophrenia pedigree. *Psychiatric Genetics*. 2004; 14(1):1–8. <https://doi.org/10.1097/00041444-200403000-00001> PMID: 15091309
30. Jagadeesan A, Gunnarsdóttir ED, Ebenesersdóttir SS, Guðmundsdóttir VB, Thordardóttir EL, Einarsdóttir MS, et al. Reconstructing an African haploid genome from the 18th century. *Nature Genetics*. 2018; 50:199–205. <https://doi.org/10.1038/s41588-017-0031-6> PMID: 29335549
31. Thatte BD, Steel M. Reconstructing pedigrees: a stochastic perspective. *Journal of Theoretical Biology*. 2008; 251(3):440–449. <https://doi.org/10.1016/j.jtbi.2007.12.004> PMID: 18249415
32. Jones OR, Wang J. COLONY: a program for parentage and sibship inference from multilocus genotype data. *Molecular Ecology Resources*. 2010; 10(3):551–555. <https://doi.org/10.1111/j.1755-0998.2009.02787.x> PMID: 21565056
33. Sheikh SI, Berger-Wolf TY, Khokhar AA, Caballero IC, Ashley MV, Chaovalitwongse W, et al. Combinatorial reconstruction of half-sibling groups from microsatellite data. *Journal of Bioinformatics and Computational Biology*. 2010; 8(02):337–356. <https://doi.org/10.1142/S0219720010004793> PMID: 20401949
34. Kirkpatrick B, Li SC, Karp RM, Halperin E. Pedigree reconstruction using identity by descent. *Journal of Computational Biology*. 2011; 18(11):1481–1493. <https://doi.org/10.1089/cmb.2011.0156> PMID: 22035331
35. He D, Wang Z, Han B, Parida L, Eskin E. IPED: inheritance path-based pedigree reconstruction algorithm using genotype data. *Journal of Computational Biology*. 2013; 20(10):780–791. <https://doi.org/10.1089/cmb.2013.0080> PMID: 24093229
36. He D, Wang Z, Parida L, Eskin E. IPED2: Inheritance path based pedigree reconstruction algorithm for complicated pedigrees. *IEEE/ACM Transactions on Computational Biology and Bioinformatics (TCBB)*. 2017; 14(5):1094–1103. <https://doi.org/10.1109/TCBB.2017.2688439> PMID: 28368828

37. Elias I, Tuller T. Reconstruction of ancestral genomic sequences using likelihood. *Journal of Computational Biology*. 2007; 14(2):216–237. <https://doi.org/10.1089/cmb.2006.0101> PMID: 17456016
38. Lee WJ, Pollin TI, O'Connell JR, Agarwala R, Schäffer AA. PedHunter 2.0 and its usage to characterize the founder structure of the Old Order Amish of Lancaster County. *BMC Medical Genetics*. 2010; 11:68. <https://doi.org/10.1186/1471-2350-11-68> PMID: 20433770
39. Elizabethtown College. Young Center for Anabaptist and Pietist Studies; 2019. Available from: <https://www.etown.edu/centers/young-center/>.
40. Agarwala R, Schäffer AA, Tomlin JF. Towards a complete North American Anabaptist Genealogy II: analysis of inbreeding. *Human Biology*. 2001; 73(4):533–545. <https://doi.org/10.1353/hub.2001.0045> PMID: 11512680
41. Coriell Institute for Medical Research. Amish Major Affective Disorders; 2019. Available from: <https://www.coriell.org/>.
42. Georgi B, Craig D, Kember RL, Liu W, Lindquist I, Nasser S, et al. Genomic view of bipolar disorder revealed by whole genome sequencing in a genetic isolate. *PLoS Genetics*. 2014; 10(3):e1004229. <https://doi.org/10.1371/journal.pgen.1004229> PMID: 24625924
43. Cannings C, Thompson E, Skolnick M. Probability functions on complex pedigrees. *Advances in Applied Probability*. 1978; 10(1):26–61. <https://doi.org/10.2307/1426718>
44. Becker A, Geiger D, Schäffer AA. Automatic Selection of Loop Breakers for Genetic Linkage Analysis. *Human Heredity*. 1998; 48(1):49–60. <https://doi.org/10.1159/000022781> PMID: 9463802
45. Beiler K. *Descendants of Christian Fisher*. 4th ed. Pequea; 2009.
46. Sinnwell J, Therneau T, Schaid D, Atkinson E, Mester C. kinship2: Pedigree Functions; 2019. Available from: <https://CRAN.R-project.org/package=kinship2>.
47. Wright S. Coefficients of inbreeding and relationship. *The American Naturalist*. 1922; 56(645):330–338. <https://doi.org/10.1086/279872>
48. Gusev A, Lowe JK, Stoffel M, Daly MJ, Altshuler D, Breslow JL, et al. Whole population, genome-wide mapping of hidden relatedness. *Genome Research*. 2009; 19(2):318–326. <https://doi.org/10.1101/gr.081398.108> PMID: 18971310
49. He D. IBD-Groupon: an efficient method for detecting group-wise identity-by-descent regions simultaneously in multiple individuals based on pairwise IBD relationships. *Bioinformatics*. 2013; 29(13):i162–i170. <https://doi.org/10.1093/bioinformatics/btt237> PMID: 23812980
50. Delaneau O, Zagury JF, Marchini J. Improved whole-chromosome phasing for disease and population genetic studies. *Nature Methods*. 2013; 10:5–6. <https://doi.org/10.1038/nmeth.2307> PMID: 23269371
51. Kelleher J, Etheridge AM, McVean G. Efficient coalescent simulation and genealogical analysis for large sample sizes. *PLoS Computational Biology*. 2016; 12(5):e1004842. <https://doi.org/10.1371/journal.pcbi.1004842> PMID: 27145223
52. The International HapMap Consortium. A second generation human haplotype map of over 3.1 million SNPs. *Nature*. 2007; 449(7164):851. <https://doi.org/10.1038/nature06258>
53. Caballero M, Seidman DN, Qiao Y, Sannerud J, Dyer TD, Lehman DM, et al. Crossover interference and sex-specific genetic maps shape identical by descent sharing in close relatives. *PLoS Genetics*. 2019; 15(12):e1007979. <https://doi.org/10.1371/journal.pgen.1007979>
54. Fu W, Zhang F, Wang Y, Gu X, Jin L. Identification of copy number variation hotspots in human populations. *American Journal of Human Genetics*. 2010; 87(4):494–504. <https://doi.org/10.1016/j.ajhg.2010.09.006> PMID: 20920665
55. Girirajan S, Dennis MY, Baker C, Malig M, Coe BP, Campbell CD, et al. Refinement and discovery of new hotspots of copy-number variation associated with autism spectrum disorder. *American Journal of Human Genetics*. 2013; 92(2):221–237. <https://doi.org/10.1016/j.ajhg.2012.12.016> PMID: 23375656
56. Kember RL, Georgi B, Bailey-Wilson JE, Stambolian D, Paul SM, Bućan M. Copy number variants encompassing Mendelian disease genes in a large multigenerational family segregating bipolar disorder. *BMC Genetics*. 2015; 16(1):27. PMID: 25887117
57. Wang K, Li M, Hadley D, Liu R, Glessner J, Grant SF, et al. PennCNV: an integrated hidden Markov model designed for high-resolution copy number variation detection in whole-genome SNP genotyping data. *Genome Research*. 2007; 17(11):1665–1674. <https://doi.org/10.1101/gr.6861907> PMID: 17921354
58. Doggett NA, Xie G, Meincke LJ, Sutherland RD, Mundt MO, Barbari NS, et al. A 360-kb interchromosomal duplication of the human HYDIN locus. *Genomics*. 2006; 88(6):762–771. <https://doi.org/10.1016/j.ygeno.2006.07.012> PMID: 16938426

59. Agarwala R, Biesecker LG, Hopkins KA, Francomano CA, Schaffer AA. Software for constructing and verifying pedigrees within large genealogies and an application to the Old Order Amish of Lancaster County. *Genome Research*. 1998; 8(3):211–221. <https://doi.org/10.1101/gr.8.3.211> PMID: 9521925
60. Johnston JJ, Kelley RI, Crawford TO, Morton DH, Agarwala R, Koch T, et al. A novel nemaline myopathy in the Amish caused by a mutation in troponin T1. *American Journal of Human Genetics*. 2000; 67(4):814–821. <https://doi.org/10.1086/303089> PMID: 10952871
61. Nelson D, Moreau C, de Vriendt M, Zeng Y, Preuss C, Vézina H, et al. Inferring transmission histories of rare alleles in population-scale genealogies. *American Journal of Human Genetics*. 2018; 103(6):893–906. <https://doi.org/10.1016/j.ajhg.2018.10.017> PMID: 30526866
62. Geyer CJ, Thompson EA. Annealing Markov chain Monte Carlo with applications to ancestral inference. *Journal of the American Statistical Association*. 1995; 90(431):909–920. <https://doi.org/10.1080/01621459.1995.10476590>
63. Gulcher JR, Kong A, Stefansson K. The role of linkage studies for common diseases. *Current Opinion in Genetics & Development*. 2001; 11(3):264–267. [https://doi.org/10.1016/S0959-437X\(00\)00188-X](https://doi.org/10.1016/S0959-437X(00)00188-X) PMID: 11377961
64. Lachance J, Tishkoff SA. SNP ascertainment bias in population genetic analyses: why it is important, and how to correct it. *Bioessays*. 2013; 35(9):780–786. <https://doi.org/10.1002/bies.201300014> PMID: 23836388
65. Payne M, Rupar CA, Siu GM, Siu VM. Amish, Mennonite, and Hutterite genetic disorder database. *Pediatrics and Child Health*. 2011; 16(3):e23. <https://doi.org/10.1093/pch/16.3.e23> PMID: 22379385
66. Pollin TI, Damcott CM, Shen H, Ott SH, Shelton J, Horenstein RB, et al. A null mutation in human APOC3 confers a favorable plasma lipid profile and apparent cardioprotection. *Science*. 2008; 322(5908):1702–1705. <https://doi.org/10.1126/science.1161524> PMID: 19074352
67. Whiffin N, Armean IM, Kleinman A, Marshall JL, Minikel EV, Goodrich JK, et al. The effect of LRRK2 loss-of-function variants in humans. *Nature Medicine*. 2020; 26(6):869–877. <https://doi.org/10.1038/s41591-020-0893-5> PMID: 32461697